CAPITAL UNIVERSITY OF SCIENCE AND TECHNOLOGY, ISLAMABAD

MHD Casson Nanofluid Flow with Cattaneo-Christov Heat Flux and Mass Transfer Over a Stretching Sheet

by

Alnaba Shoukat

A thesis submitted in partial fulfillment for the degree of Master of Philosophy

in the

Faculty of Computing
Department of Mathematics

2022

*I dedicate my dissertation work to my **family** and dignified **teachers**. A special feeling of gratitude to my loving parents who have supported me in my studies.*

CERTIFICATE OF APPROVAL

MHD Casson Nanofluid Flow with Cattaneo-Christov Heat Flux and Mass Transfer Over a Stretching Sheet

by

Alnaba Shoukat

(MMT191029)

THESIS EXAMINING COMMITTEE

(a)	External Examiner	Dr. Muhammad Kamran	CIIT, Wah Cantt
(b)	Internal Examiner	Dr. Muhammad Sabeel Khan	CUST, Islamabad
(c)	Supervisor	Dr. Muhammad Sagheer	CUST, Islamabad

Dr. Muhammad Sagheer
Thesis Supervisor
December, 2022

Dr. Muhammad Sagheer
Head
Dept. of Mathematics
December, 2022

Dr. M. Abdul Qadir
Dean
Faculty of Computing
December, 2022

Author's Declaration

I, **Alnaba Shoukat**, hereby state that my MPhil thesis titled "**MHD Casson Nanofluid Flow with Cattaneo-Christov Heat Flux and Mass Transfer Over a Stretching Sheet**" is my own work and has not been submitted previously by me for taking any degree from Capital University of Science and Technology, Islamabad or anywhere else in the country/abroad.

At any time if my statement is found to be incorrect even after my graduation, the University has the right to withdraw my MPhil Degree.

(Alnaba Shoukat)

Registration No: MMT191029

Plagiarism Undertaking

I solemnly declare that research work presented in this thesis titled "**MHD Casson Nanofluid Flow with Cattaneo-Christov Heat Flux and Mass Transfer Over a Stretching Sheet**" is solely my research work with no significant contribution from any other person. Small contribution/help wherever taken has been dully acknowledged and that complete thesis has been written by me.

I understand the zero tolerance policy of the HEC and Capital University of Science and Technology towards plagiarism. Therefore, I as an author of the above titled thesis declare that no portion of my thesis has been plagiarized and any material used as reference is properly referred/cited.

I undertake that if I am found guilty of any formal plagiarism in the above titled thesis even after award of MPhil Degree, the University reserves the right to withdraw/revoke my MPhil degree and that HEC and the University have the right to publish my name on the HEC/University website on which names of students are placed who submitted plagiarized work.

(Alnaba Shoukat)

Registration No: MMT191029

Acknowledgement

Allah the Compassionate, the Merciful. O my Lord! open for me my chest and eases my task for me and lose the knot (the defect) from my tongue that they may understand my speech. First of all I am thankful to **Almighty Allah**, the most merciful, all knowing, who gave me courage and strength to carry out the demanding research for this thesis and provided me the opportunity to complete this humble contribution towards knowledge.

Work on this thesis would not have been possible without contributions, support and encouragement from many people. Firstly, I would like to thank my respected supervisor, **Dr. Muhammad Sagheer**, whose timely advice and guidance enabled me to complete this research study which has been a great test for me as a beginner to this research problem. I can never forget his politeness, precious suggestions and valuable advice. I pray to Allah Almighty to give him strength to continue his guidance to the new students of this field in the right direction.

I owe my deepest gratitude to my family for being there for me and for always believing in me. I would really appreciate the endless efforts of my **parents** and **sisters** to bring me at such a point to enable me to feel proud of myself. Without their co-operation and support all this would have been impossible. I am thankful to my respectable father who guided and supported me at every step of my life. Finally, I am thankful to all my lovely **friends** for their appreciation and encouragement.

(Alnaba Shoukat)

Abstract

This thesis numerically investigates the influence of Cattaeno-Christov heat flux and chemical reaction of the flow past a stretching sheet through a porous medium. The partial differential equations governing the flow problem are converted to ordinary differential equations using similarity transformation. In order to solve the ODEs, the shooting technique is implemented in MATLAB. The influence of physical parameters such as magnetic field parameter, Prandtl number, thermophoresis parameter, Brownian motion parameter, relaxation time parameter and chemical reaction parameter on the velocity profile, temperature distribution, concentration profile, skin friction coefficient, Nusselt number and Sherwood number are studied and presented in graphical and tabular forms. The results show that increasing the values of Casson fluid parameter, the velocity profile decreases while the temperature profile increases. Enhancing the values of the relaxation time parameter, the temperature profile is decreased. Due to the ascending values of the chemical reaction parameter, the numerical values of the local Nusselt number are decreased while the local Sherwood number is increased.

Contents

List of Figures

List of Tables

Abbreviations

IVPs	Initial value problems
MHD	Magnetohydrodynamics
ODEs	Ordinary differential equations
PDEs	Partial differential equations
RK	Runge-Kutta

Symbols

μ	Viscosity
ρ	Density
ν	Kinematic viscosity
τ	Stress tensor
k	Thermal conductivity
α	Thermal diffusivity
σ	Electrical conductivity
u	x-component of fluid velocity
v	y-component of fluid velocity
B_0	Magnetic field constant
k_1	Permeability constant
a	Stretching constant
λ	Relaxation time constant
T_w	Temperature of the wall
T_∞	Ambient temperature of the nanofluid
T	Temperature
C_∞	Ambient concentration
C	Concentration
C_w	Nanoparticles concentration at the stretching surface
q_r	Radiative heat flux
q	Heat generation constant
q_w	Heat flux
q_m	Mass flux

σ^*	Stefan Boltzmann constant
k^*	Absorption coefficient
ψ	Stream function
ζ	Similarity variable
C_f	Skin friction coefficient
Nu	Nusselt number
Nu_x	Local Nusselt number
Sh	Sherwood number
Sh_x	Local Sherwood number
Re	Reynolds number
Re_x	Local Reynolds number
R	Thermal radiation parameter
M	Magnetic parameter
K	Permeability parameter
Pr	Prandtl number
γ_1	Relaxation time parameter
γ_2	Chemical reaction parameter
Nb	Brownain motion parameter
Nt	Thermophoresis parameter
Sc	Schmidt number
f	Dimensionless velocity
θ	Dimensionless temperature
ϕ	Dimensionless concentration

Chapter 1

Introduction

In general, the conventional fluids utilized in many industrial processes, such as water, ethylene glycol, and engine oil, are poor heat conductors due to their low thermal conductivities. If a little portion of nanoparticles (such as Cu, Ag, TiO_2 and Al_2O_3) is immersed into a conventional fluid, a new category of fluids is obtained which is called nanofluids [1]. Nanofluids paved a new pathway to innovations in the improvement of the characteristics of heat transfer. There is a wide variety of nanoparticles which are categorised according to their size, shape, thermal and electrical conductivity and heat transfer abilities. Yacob et al. [2] conducted an investigation of a nanofluid's boundary layer flow across a stretching/shrinking sheet with a convective boundary condition. The impact of heat generation or absorption on the constant free convection flow of a nanofluid across a perforated vertical plate with vacuum or injection was examined by Chamkha and El-Kabeir [3]. They used an implicit finite difference approach for the solution of problem. Mahdy et al. [4] tested the influence of a stretched sheet on mixed convection flow and rate of heat transfer in nanofluids. In comparison to pure water, they discovered that nanofluids had a higher rate of heat transfer at their thermal boundary layer and vertical stretching surface. Nanofluids have various applications in industrial devices, heat exchanger [5], drug delivery, medicines, car radiators, cooling of heat exchanging equipments, transformer oil cooling, electronic cooling [6, 7]. The diameter of the suspended nanoparticle varies between

1 to 100nm. There appears a dramatic boost in the thermophysical properties of the conventional fluid when the nanoparticle are suspended in it.

In 2006, Buongiorno [8] presented a detailed discussion on convective transport system in nanofluids. He encountered the fact that Brownian diffusion and thermophoresis are the primary mechanisms for the improvement rate of heat transfer and deduced that the immense fluctuations of temperature in the boundary layer zone result in a noticeable reduction in fluid's viscosity which as a consequence leads to a rise in the coefficient of heat transfer.

Tiwari and Das [9] in 2007, further devised a model for the examination of nanofluid and heat transfer within a two-sided lid-driven square cavity and analyzed the role of nanoparticle volume fraction. They emphasized on the prime role of nanoparticle volume fraction for evaluating the impact of nanoparticles in the fluid flow and rate of heat transfer. Yang et al. [10] mentioned that, the thermal conductivity of nanofluid relies highly on nanoparticle's volume fraction and their different properties such as diameter and shape.

Khan and Pop [11] were able to generate first ever paper work on laminar flow of nanofluids over a stretching sheet emphasizing that the behaviour can also be well observed in nanofluids. Hady et al. [12] performed similar experiments depicting behaviours of nanofluids over a stretching sheet. Wang [13] were the first who theoretically and experimentally noted down the flow towards a shrinking sheet. Out of many significant characteristics, the most advanceed to grasp interest are MHD and thermal radiation affects on nanofluids. Nadeem et al. [14] used honotopy method to observe two dimensional flow of heat transfer considering Williamson nanofluids, these nanofluids are various non-eleastic fluids. His work was followed by Prasannakumara et al. [15] analysing chemical activity on a porous medium.

One of the fluids that defies Newton's laws is the Casson fluid, which may be beneficial in applications involving blood flow. Vijayaragavan and Karthikeyan [16] gave a thorough discussion of the MHD Casson fluid included the Hall, Dufour and thermal radiation properties. For the MHD flow of Casson liquid, Hayat et al. [17] examined the influence of the Soret and Dufour effects. The Casson fluid has been used in the creation of polymers, silicon suspensions, and printer ink [18].

Moreover, Pramanik [19] has studied the heat transfer in the Casson nanofluid flow by including the thermal radiation. Recent research [20–22] have described various elements of these flows utilizing the Casson fluid. Kamran et al. [23] reported an analysis of an MHD Casson nanofluid flow considering the Joule heating and slip boundary conditions.

Magnetohydrodynamics is a topic related to fluid mechanics with an applied magnetic field and classical electromagnetism. It has numerous engineering uses, including in welding, solar energy collectors, reactor cooling and crystal formation. Sarveshanand and Singh [24] carry out the two-dimensional, electrically conducting free convective fluid flow between porous plates. Madhura and Iyengar [25] have explored the mass and heat energy effects on MHD nano-fluid flow over a stationary/moving plate that is drenched in a spongy medium. Mabood et al. [26] being the former in this field investigated MHD boundary layer flow over a nonlinear stretching sheet. MHD stagnation point was theoretically and experimentally targeted by Ibrahim et al. [27]. Bhatti et al. [28] critically evaluated Reynolds number relation to magnetic field. This work was taken on experimental basis by Xuan and Li. [29] who took volume percentage into consideration this time. The Jha and Aina [30] for MHD natural convention flow travelling through a vertical microchannel by taking induced magnetic field into account reveal a closed-form of the mixture. They claimed that as the magnetic Prandtl number and Hartmann number increase, the induced magnetic field acts as an increasing function. The presentation of heat tranfer on two phase model with affects of MHD and thermal radiation was made in its earliest form by Sheikhouslani et al. [31]. Magnetic field parameters, Brownain motion, heat production and thermal profile where evaluated by Poply et al. [32] under the effects of MHD. Chamkha and Aly [33] successfully described MHD boundary layer flow with convective slip flow under the effects of heat. Ahmed et al. [34] and Ganga et al. [35] also contributed sinificantly by considering magnetohydrodynamics in the fluid flow problems.

Porous medium is a material having pores, which means that the pores are fully connected and filled with the fluid, and fluid may flow through the voids. The use of porous media with nanofluid increases the efficiency of thermal systems

because porous media increases contact surface area while nanoparticles increase thermal conductivity [36]. The characteristics of porosity are examined by Sumirat et al. [37]. In porous media, heat transport and nanofluid flow were addressed by Mahdi et al. [38].
Heterogeneous and homogeneous systems are two types of chemical reactions. As discussed by Magyari and Chamkha [39], the concentration rate in most chemical reaction processes is determined by the species itself. Das [40] demonstrated the impact of chemical reactions and radiation on the heat and mass exchange along with the MHD flow. Chamkha and Rashad [41] analyzed the effect of chemical reactions on MHD flow when heat is produced or absorbed by a uniform vertical permeable surface.

1.1 Thesis Contributions

The present analysis is dedicated to the numerical solution of mathematical model governing an MHD Casson nanofluid flow with Cattaneo-Christov heat flux model and chemical reaction. By using appropriate transformations, the proposed nonlinear PDEs are changed into an ODE system. The shooting technique is used to determine the numerical values of the nonlinear ODEs. The numerically obtained results are computed by using MATLAB. Graphs and tables have been used to discuss the effects of important factors on the distributions of velocity $f'(\zeta)$, temperature $\theta(\zeta)$ and concentation $\phi(\zeta)$ as well as the skin friction coefficient C_f, local Nusselt number Nu_x and local Sherwood number Sh_x.

1.2 Layout of Thesis

A brief overview of the contents of the thesis is provided below.

Chapter 2 includes some basic definitions and terminologies, which are useful to understand the concepts discussed later on.

Chapter 3 provides the proposed analytical study of MHD Casson nanofluid flow, heat transmission and mass transfer across a stretched sheet. The numerical results of the governing flow equations are derived by the shooting technique.

Chapter 4 extends the proposed model flow discussed in Chapter 3 by including the impacts of Cattaneo-Christov heat flux model and chemical reaction.

Chapter 5 provides the concluding remarks of the thesis.

References used in the thesis are mentioned in **Biblography**.

Chapter 2

Preliminaries

Basic definitions and guiding principles are presented in this chapter. These will be useful in the succeeding chapters.

2.1 Some Basic Terminologies

Definition 2.1.1 (Fluid)
"A fluid is a substance that deforms continuously under the application of a shear (tangential) stress no matter how small the shear stress may be." [42]

Definition 2.1.2 (Fluid Mechanics)
"Fluid mechanics is that branch of science which deals with the behavior of the fluid (liquids or gases) at rest as well as in motion." [43]

Definition 2.1.3 (Fluid Dynamics)
"The study of the motion of gases, liquids and plasmas from one place to another. It has many useful applications which are use in our daily life such as, mass flow rate of petroleum passing through pipelines, prediction of weather, etc." [43]

Definition 2.1.4 (Fluid Statics)

"The study of fluid at rest is called fluid statics." [43]

Definition 2.1.5 (Viscosity)

"Viscosity is defined as the property of a fluid which offers resistance to the movement of one layer of fluid over another adjacent layer of the fluid. Mathematically,

$$\mu = \frac{\tau}{\frac{\partial u}{\partial y}},$$

where μ is viscosity coefficient, τ is shear stress and $\frac{\partial u}{\partial y}$ represents the velocity gradient." [43]

Definition 2.1.6 (Kinematic Viscosity)

"It is defined as the ratio between the dynamic viscosity and density of fluid. It is denoted by ν. Mathematically,

$$\nu = \frac{\mu}{\rho}.\text{" [43]}$$

Definition 2.1.7 (Thermal Conductivity)

"The Fourier heat conduction law states that the heat flow is proportional to the temperature gradient. The coefficient of proportionality is a material parameter known as the thermal conductivity which may be a function of a number of variables." [44]

2.2 Types of Fluid

Definition 2.2.1 (Newtonian Fluid)

"A real fluid, in which the shear stress is directly proportional to the rate of shear strain (or velocity gradient), is known as a Newtonian fluid." [43]

Definition 2.2.2 (Non-Newtonian Fluid)

"A real fluid in which the shear stress is not directly proportional to the rate of shear strain (or velocity gradient), is known as a non-Newtonian fluid.

$$\tau_{xy} \propto \left(\frac{du}{dy}\right)^m; \qquad m \neq 1,$$
$$\tau_{xy} = \mu\left(\frac{du}{dy}\right)^m." \text{ [43]}$$

Definition 2.2.3 (Ideal Fluid)

"A fluid, which is incompressible and has no viscosity, is known as an ideal fluid. Ideal fluid is only an imaginary fluid as all the fluids, which exist, have some viscosity." [43]

Definition 2.2.4 (Real Fluid)

"A fluid, which possesses viscosity, is known as a real fluid. In actual practice, all the fluids are real fluids." [43]

Definition 2.2.5 (Magnetohydrodynamics)

"Magnetohydrodynamics(MHD) is concerned with the mutual interaction of fluid flow and magnetic fields. The fluids in question must be electrically conducting and non-magnetic, which limits us to liquid metals, hot ionised gases (plasmas) and strong electrolytes." [45]

2.3 Types of Flow

Definition 2.3.1 (Steady Flow)

"If the flow characteristics such as depth of flow, velocity of flow, rate of flow at any point in open channel flow do not change with respect to time, the flow is said to be steady flow. Mathematically,

$$\frac{\partial Q}{\partial t} = 0,$$

where Q is any fluid property.” [43]

Definition 2.3.2 (Unsteady Flow)

“If at any point in open channel flow, the velocity of flow, depth of flow or rate of flow changes with respect to time, the flow is said to be unsteady. Mathematically,

$$\frac{\partial Q}{\partial t} \neq 0,$$

where Q is any fluid property.” [43]

Definition 2.3.3 (Compressible Flow)

“Compressible flow is that type of flow in which the density of the fluid changes from point to point or in other words the density (ρ) is not constant for the fluid, Mathematically,

$$\rho \neq k,$$

where k is constant.” [43]

Definition 2.3.4 (Incompressible Flow)

“Incompressible flow is that type of flow in which the density is constant for the fluid. Liquids are generally incompressible while gases are compressible, Mathematically,

$$\rho = k,$$

where k is constant.” [43]

Definition 2.3.5 (Rotational Flow)

“Rotational flow is that type of flow in which the fluid particles while flowing along stream-lines, also rotate about their own axis.” [43]

Definition 2.3.6 (Irrotational Flow)

"Irrotational flow is that type of flow in which the fluid particles while flowing along stream-lines, do not rotate about their own axis then this type of flow is called irrotational flow." [43]

Definition 2.3.7 (Internal Flow)

"Flows completely bounded by a solid surfaces are called internal or duct flows." [42]

Definition 2.3.8 (External Flow)

"Flows over bodies immersed in an unbounded fluid are said to be an external flow." [42]

2.4 Modes of Heat Transfer

Definition 2.4.1 (Heat Transfer)

"Heat transfer is a branch of engineering that deals with the transfer of thermal energy from one point to another within a medium or from one medium to another due to the occurrence of a temperature difference." [44]

Definition 2.4.2 (Conduction)

"Due to collision of molecules in the contact form, heat is transferred from one object to another object. This phenomenon is called conduction. Such type of heat transfer occurs in the solids." [44]

Definition 2.4.3 (Convection)

"Convection heat transfer is usually defined as energy transport effected by the motion of a fluid. The convection heat transfer between two dissimilar media is governed by Newtons law of cooling." [44]

Definition 2.4.4 (Thermal Radiation)

"Thermal radiation is defined as radiant (electromagnetic) energy emitted by a medium and is solely to the temperature of the medium." [44]

2.5 Dimensionless Numbers

Definition 2.5.1 (Prandtl Number)

"It is the ratio between the momentum diffusivity ν and thermal diffusivity α. Mathematically, it can be defined as

$$Pr = \frac{\nu}{\alpha} = \frac{\frac{\mu}{\rho}}{\frac{k}{C_p\rho}}$$

$$Pr = \frac{\mu C_p}{k}$$

where μ represents the dynamic viscosity, Cp denotes the specific heat and k stands for thermal conductivity. The relative thickness of thermal and momentum boundary layer is controlled by Prandtl number. For small Pr, heat distributed rapidly corresponds to the momentum." [42]

Definition 2.5.2 (Eckert Number)

"It is the dimensionless number used in continuum mechanics. It describes the relation between flows and the boundary layer enthalpy difference and it is used for characterized heat dissipation. Mathematically,

$$Ec = \frac{u^2}{C_p \nabla T}$$

where C_p denotes the specific heat." [42]

Definition 2.5.3 (Skin Friction Coefficient)

"The steady flow of an incompressible gas or liquid in a long pipe of internal D.

The mean velocity is denoted by u_w. The skin friction coefficient can be defined as

$$C_f = \frac{2\tau_0}{\rho u_w^2}$$

where τ_0 denotes the wall shear stress and ρ is the density.” [46]

Definition 2.5.4 (Nusselt Number)

“The hot surface is cooled by a cold fluid stream. The heat from the hot surface, which is maintained at a constant temperature, is diffused through a boundary layer and convected away by the cold stream. Mathematically,

$$Nu = \frac{qL}{k}$$

where q stands for the convection heat transfer, L for the characteristic length and k stands for thermal conductivity.” [47]

Definition 2.5.5 (Sherwood Number)

“It is the nondimensional quantity which shows the ratio of the mass transport by convection to the transfer of mass by diffusion. Mathematically:

$$Sh = \frac{kL}{D},$$

where L is characteristics length, D is the mass diffusivity and k is the mass transfer coeffcient.” [48]

Definition 2.5.6 (Reynolds Number)

“It is defined as the ratio of inertia force of a flowing fluid and the viscous force of the fluid. Mathematically,

$$Re = \frac{VL}{\nu},$$

where V denotes the free stream velocity, L is the characteristic length and ν stands for kinematic viscosity.” [43]

2.6 Governing Laws

Continuity Equation

"The principle of conservation of mass can be stated as the time rate of change of mass fixed volume is equal to the net rate of flow of mass across the surface. Mathematically, it can be written as

$$\frac{\partial \rho}{\partial t} + \nabla.(\rho \mathbf{u}) = 0.\text{" [44]}$$

Momentum Equation

"The momentum equation states that the time rate of change of linear momentum of a given set of particles is equal to the vector sum of all the external forces acting on the particles of the set, provided Newtons Third Law of action and reaction governs the internal forces. Mathematically, it can be written as:

$$\frac{\partial}{\partial t}(\rho \mathbf{u}) + \nabla.[(\rho \mathbf{u})\mathbf{u}] = \nabla.\mathbf{T} + \rho g.\text{" [44]}$$

Energy Equation

"The law of conservation of energy states that the time rate of change of the total energy is equal to the sum of the rate of work done by the applied forces and change of heat content per unit time.

$$\frac{\partial \rho}{\partial t} + \nabla.\rho \mathbf{u} = -\nabla.\mathbf{q} + Q + \phi,$$

where ϕ is the dissipation function." [44]

2.7 Shooting Method

To elaborate the shooting method, take into account the subsequent nonlinear boundary value problem.

$$\left.\begin{aligned} &h'''(\zeta) = h(\zeta)h''(\zeta) + h'^2(\zeta) - h(\zeta)h'(\zeta) \\ &h(0) = 0, \qquad h'(0) = 1, \qquad h'(J) = 0. \end{aligned}\right\} \tag{2.1}$$

To reduce the order of the above BVP, introduce the following notations.

$$h = W_1, \qquad h' = W_1' = W_2, \qquad h'' = W_2' = W_3, \qquad h''' = W_3'. \tag{2.2}$$

The system of first order ODEs that results from the conversion of (2.1) is as follows.

$$W_1' = W_2, \qquad W_1(0) = 0. \tag{2.3}$$

$$W_2' = W_3, \qquad W_2(0) = 1. \tag{2.4}$$

$$W_3' = W_1W_3 + 2W_2^2 - W_1W_2, \qquad W_3(0) = s, \tag{2.5}$$

where s is the missing initial condition which will be guessed.
The RK-4 method will be used to numerically solve the above IVP. Choose the missing condition s in such a way that.

$$W_2(J, s) = 0. \tag{2.6}$$

For convenience, now onward $W_2(J, s)$ will be denoted by $W_2(s)$.

$$W_2(s) = 0. \tag{2.7}$$

The above equation can be solved by using Newton's method with the following iterative formula.

$$s^{(n+1)} = s^{(n)} - \frac{W_2(s^{(n)})}{\left(\frac{\partial W_2(s)}{\partial s}\right)^{(n)}}, \tag{2.8}$$

To find $\left(\frac{\partial W_2(s)}{\partial s}\right)^n$, introduce the following notations.

$$\frac{\partial W_1}{\partial s} = W_4, \qquad \frac{\partial W_2}{\partial s} = W_5, \qquad \frac{\partial W_3}{\partial s} = W_6. \tag{2.9}$$

As a result of these new notations the Newton's iterative scheme, will then get the form.

$$s^{n+1} = s^n - \frac{W_2(s^n)}{W_5(s^n)}. \tag{2.10}$$

Now differentiating the system of three first order ODEs (2.3)-(2.5) with respect to s, we get another system of ODEs, as follows.

$$W_4' = W_5, \qquad W_4(0) = 0. \tag{2.11}$$

$$W_5' = W_6, \qquad W_5(0) = 0. \tag{2.12}$$

$$W_6' = W_4W_3 + W_1W_6 + 4W_2W_5 - W_4W_2 - W_1W_5, \qquad W_6(0) = 1. \tag{2.13}$$

Writing all the six ODEs (2.3), (2.4), (2.5), (2.11), (2.12) and (2.13) together, we have the following initial value problem.

$$\begin{aligned}
W_1' &= W_2, && W_1(0) = 0. \\
W_2' &= W_3, && W_2(0) = 1. \\
W_3' &= W_1W_3 + 2W_2^2 - W_1W_2, && W_3(0) = s. \\
W_4' &= W_5, && W_4(0) = 0. \\
W_5' &= W_6, && W_5(0) = 0. \\
W_6' &= W_4W_3 + W_1W_6 + 4W_2W_5 - W_4W_2 - W_1W_5, && W_6(0) = 1.
\end{aligned}$$

The above system together will be solved numerically by RK-4 method. The stopping criteria for the Newton's technique is set as,

$$\mid W_2(s) \mid < \epsilon,$$

where $\epsilon > 0$ is an arbitrarily small positive number.

Chapter 3

MHD Heat and Mass Transfer Casson Nanofluid Flow past a Stretching Sheet

3.1 Introduction

In this chapter, consideration has been given to the numerical analysis of MHD Casson nanofluid flow past a stretching sheet, saturated in a porous medium in the presence of magnetic field and thermal radiation. The governing nonlinear PDEs are converted into a system of dimensionless ODEs by utilizing the appropriate transformations. The numerical solution of ODEs is obtaind by applying shooting method. At the end of this chapter, the numerical solution for various parameters is discussed for the dimensionless velocity $f'(\zeta)$, temperature distribution $\theta(\zeta)$ and concentration distribution $\phi(\zeta)$. Investigation of the obtained numerical results are given through tables and graphs. This chapter provides a detailed review of the work presented by Kho et al. [49]

3.2 Mathematical Modeling

In this model we consider the $2D$ MHD flow of a stretched sheet is passed by the Casson nanofluid with $y = 0$ has been investigated. The flow is considered along y-axis with $y > 0$. It is assumed that the variable stretching velocity, of the nanofluid flow are $U_w(x)$=ax. At the stretching surface, the wall temperature T_w and the nanoparticles concentration C_w have been considered to be constant. The ambient temperature and ambient concentration are indicated by T_∞ and C_∞ respecetively.

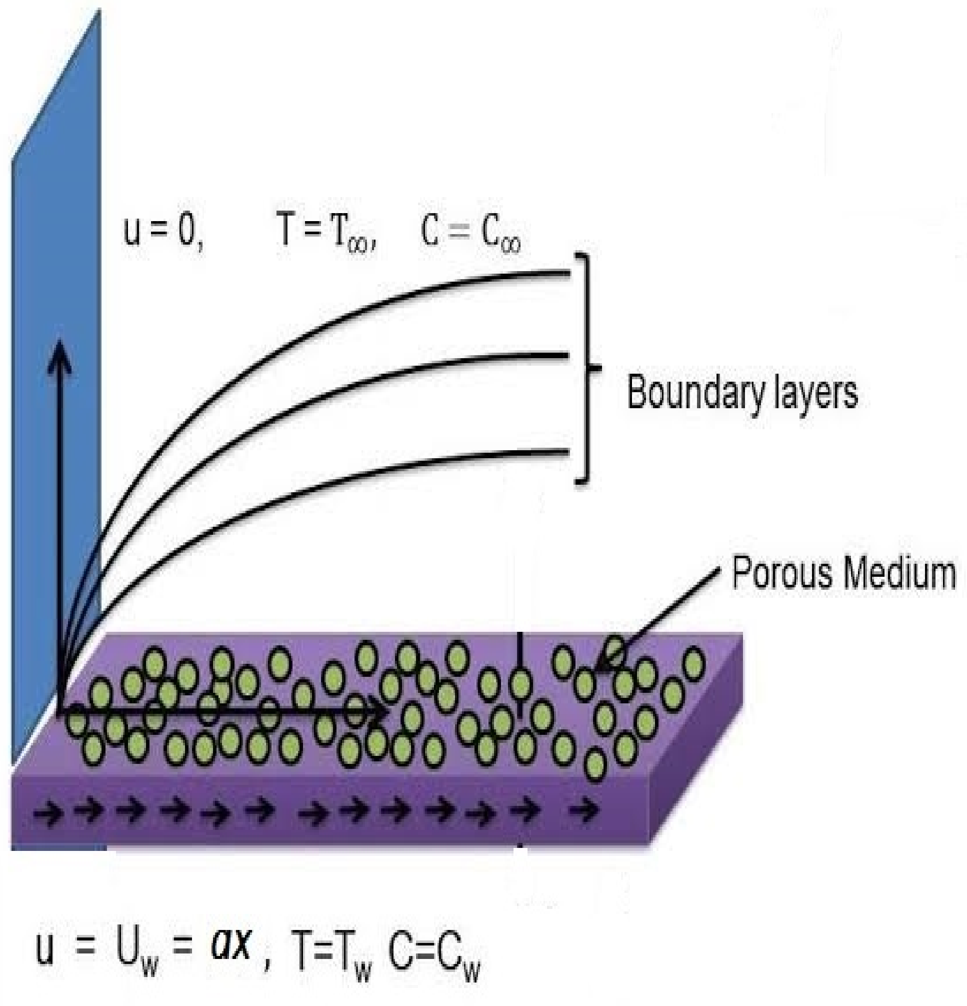

FIGURE 3.1: Systematic representation of physical model.

The flow is described by the following set of equations.

$$\frac{\partial u}{\partial x}+\frac{\partial v}{\partial y}=0, \tag{3.1}$$

$$u\frac{\partial u}{\partial x}+v\frac{\partial u}{\partial y}=\nu\left(1+\frac{1}{\beta}\right)\frac{\partial^2 u}{\partial y^2}-\frac{\nu}{k_1}u-\frac{\sigma B_0^2}{\rho}u, \tag{3.2}$$

$$u\frac{\partial T}{\partial x}+v\frac{\partial T}{\partial y}=\alpha\left(\frac{\partial^2 T}{\partial y^2}\right)+\tau\left[D_B\frac{\partial C}{\partial y}\frac{\partial T}{\partial y}+\frac{D_T}{T_\infty}\left(\frac{\partial T}{\partial y}\right)^2\right]-\frac{1}{(\rho C_p)}\left(\frac{\partial q_r}{\partial y}\right), \tag{3.3}$$

$$u\frac{\partial C}{\partial x}+v\frac{\partial C}{\partial y}=D_B\frac{\partial^2 C}{\partial y^2}+\left(\frac{D_T}{T_\infty}\right)\frac{\partial^2 T}{\partial y^2}. \tag{3.4}$$

The associated BCs have been taken as.

$$\left.\begin{array}{l} u=U_w(x)=ax, \quad v=0, \quad T=T_w, \quad C=C_w, \quad at \quad y=0, \\ u\to 0, \quad v\to 0, \quad T\to T_\infty, \quad C\to C_\infty, \quad as \quad y\to\infty. \end{array}\right\} \tag{3.5}$$

In the above model, x is the direction around the sheet, the direcetion perpendicular to the sheet is y, u and v are the xy-direction horizontal and vertical velocity component.

Radiative heat flux and heat generation constants are q_r and q. The radiative heat flux is given by

$$q_r=-\frac{4\sigma^*}{3k^*}\frac{\partial T^4}{\partial y},$$

where the Stefan-Boltzman constant is σ^* and the absorption coefficient is k^*. If the temperature difference is very small, the Taylor series can be used to expend the temperature T^4 around T_∞, as follows.

$$T^4=T_\infty^4+4T_\infty^3(T-T_\infty)+6T_\infty^2(T-T_\infty)^2+...$$

The higher order terms are ignored, and we have

$$\begin{aligned} T^4 &= T_\infty^4+4T_\infty^3(T-T_\infty) \\ &= T_\infty^4+4T_\infty^3T-4T_\infty^4 \\ &= 4T_\infty^3T-3T_\infty^4. \end{aligned}$$

The following similarity transformation are employed by [49] for the conversion of the mathematical model (3.1)-(3.4) into the system of ODEs.

$$\left.\begin{aligned} \psi(x,y) &= (a\nu)^{\frac{1}{2}} x f(\zeta), & \theta(\zeta) &= \frac{T-T_\infty}{T_w-T_\infty}, \\ \zeta &= \left(\frac{a}{\nu}\right)^{\frac{1}{2}} y, & \phi(\zeta) &= \frac{C-C_\infty}{C_w-C_\infty}, \end{aligned}\right\} \tag{3.6}$$

where ψ denotes the stream function.

The detailed procedure for the conversion of (3.1)-(3.4) into the dimensionless form has been discussed below.

$$u = \frac{\partial \psi}{\partial y}.$$

$$\frac{\partial u}{\partial x} = \frac{\partial}{\partial x}\left(\frac{\partial \psi}{\partial y}\right).$$

$$\frac{\partial \psi}{\partial y} = \frac{\partial}{\partial y}\left((a\nu)^{\frac{1}{2}} x f(\zeta)\right)$$

$$= (a\nu)^{\frac{1}{2}} x f'(\zeta)\frac{\partial \zeta}{\partial y}.$$

$$\frac{\partial \zeta}{\partial y} = \left(\frac{a}{\nu}\right)^{\frac{1}{2}}$$

$$= (a\nu)^{\frac{1}{2}} x f'(\zeta)\left(\frac{a}{\nu}\right)^{\frac{1}{2}}.$$

$$\frac{\partial \psi}{\partial y} = a x f'(\zeta).$$

$$u = a x f'(\zeta). \tag{3.7}$$

$$\frac{\partial u}{\partial x} = \frac{\partial}{\partial x}\left(a x f'(\zeta)\right)$$

$$= a f'(\zeta)\frac{\partial}{\partial x}(x).$$

$$\frac{\partial u}{\partial x} = a f'(\zeta). \tag{3.8}$$

$$v = -\frac{\partial \psi}{\partial x}.$$

$$\frac{\partial v}{\partial y} = -\frac{\partial}{\partial y}\left(\frac{\partial \psi}{\partial x}\right).$$

$$\frac{\partial \psi}{\partial x} = \frac{\partial}{\partial x}\left((a\nu)^{\frac{1}{2}} x f(\zeta)\right)$$

$$= (a\nu)^{\frac{1}{2}} f(\zeta).$$

$$
\begin{aligned}
v &= -(a\nu)^{\frac{1}{2}} f(\zeta). && (3.9)\\
\frac{\partial v}{\partial y} &= \frac{\partial}{\partial y}\left(-(a\nu)^{\frac{1}{2}} f(\zeta)\right)\\
&= -(a\nu)^{\frac{1}{2}} f'(\zeta)\left(\frac{a}{\nu}\right)^{\frac{1}{2}}\\
&= -af'(\zeta). && (3.10)
\end{aligned}
$$

Equation (3.1) is satisfied by using (3.8) and (3.10), as follows

$$
\frac{\partial u}{\partial x} + \frac{\partial v}{\partial y} = af'(\zeta) - af'(\zeta) = 0. \tag{3.11}
$$

Now, for the momentum equation (3.2), the following derivatives are required.

$$
\begin{aligned}
\frac{\partial u}{\partial y} &= \frac{\partial}{\partial y}(axf'(\zeta))\\
&= axf''(\zeta)\frac{\partial \zeta}{\partial y}\\
&= axf''(\zeta)\left(\frac{a}{\nu}\right)^{\frac{1}{2}}. && (3.12)\\
\frac{\partial^2 u}{\partial y^2} &= axf'''(\zeta)\left(\frac{a}{\nu}\right)^{\frac{1}{2}} \frac{\partial \zeta}{\partial y}\\
&= axf'''(\zeta)\left(\frac{a}{\nu}\right)^{\frac{1}{2}}\left(\frac{a}{\nu}\right)^{\frac{1}{2}}\\
&= \frac{a^2 x}{\nu} f'''(\zeta). && (3.13)\\
u\frac{\partial u}{\partial x} &= (axf'(\zeta))(af'(\zeta))\\
&= a^2 x f'^2(\zeta). && (3.14)\\
v\frac{\partial u}{\partial y} &= \left(-(a\nu)^{\frac{1}{2}} f(\zeta)\right)\left(axf''(\zeta)\left(\frac{a}{\nu}\right)^{\frac{1}{2}}\right)\\
&= -(a\nu)^{\frac{1}{2}} f(\zeta) axf''(\zeta)\left(\frac{a}{\nu}\right)^{\frac{1}{2}}\\
&= -a^2 x f(\zeta) f''(\zeta). && (3.15)
\end{aligned}
$$

Using (3.14) and (3.15), the left side of (3.2) becomes

$$
\begin{aligned}
u\frac{\partial u}{\partial x} + v\frac{\partial u}{\partial y} &= a^2 x f'^2(\zeta) - a^2 x f(\zeta) f''(\zeta)\\
&= a^2 x\left(f'^2(\zeta) - f(\zeta) f''(\zeta)\right). && (3.16)
\end{aligned}
$$

Using (3.7) and (3.13), the right side of (3.2) becomes,

$$
\begin{aligned}
&\nu\left(1+\frac{1}{\beta}\right)\frac{\partial^2 u}{\partial y^2}-\frac{\nu}{k_1}u-\frac{\sigma B_o^2}{\rho}u\\
&=\nu\left(1+\frac{1}{\beta}\right)\left(\frac{a^2x}{\nu}f'''(\zeta)\right)-\frac{\nu}{k_1}axf'(\zeta)-\frac{\sigma B_o^2}{\rho}axf'(\zeta),\\
&=\left(1+\frac{1}{\beta}\right)\left(a^2xf'''(\zeta)\right)-\frac{\nu}{k_1}axf'(\zeta)-\frac{\sigma B_o^2}{\rho}axf'(\zeta). \qquad (3.17)
\end{aligned}
$$

Comparing (3.16) and (3.17), the dimensionless form of (3.2) can be written as:

$$
\begin{aligned}
& a^2x\left(f'^2(\zeta)-f(\zeta)f''(\zeta)\right)=\left(1+\frac{1}{\beta}\right)\left(a^2xf'''(\zeta)\right)-\frac{\nu}{k_1}axf'(\zeta)-\frac{\sigma B_o^2}{\rho}axf'(\zeta).\\
\Rightarrow\ & a^2x\left(f'^2(\zeta)-f(\zeta)f''(\zeta)\right)=a^2x\left(\left(\frac{1+\beta}{\beta}\right)f'''(\zeta)-\frac{\nu}{k_1a}f'(\zeta)-\frac{\sigma B_o^2}{\rho a}f'(\zeta)\right).\\
\Rightarrow\ & \frac{a^2x}{a^2x}\left(f'^2(\zeta)-f(\zeta)f''(\zeta)\right)=\left(\frac{1+\beta}{\beta}\right)f'''(\zeta)-\frac{\nu}{k_1a}f'(\zeta)-\frac{\sigma B_o^2}{\rho a}f'(\zeta).\\
\Rightarrow\ & f'^2(\zeta)-f(\zeta)f''(\zeta)=\left(\frac{1+\beta}{\beta}\right)f'''(\zeta)-\frac{\nu}{k_1a}f'(\zeta)-\frac{\sigma B_o^2}{\rho a}f'(\zeta).\\
\Rightarrow\ & \left(\frac{1+\beta}{\beta}\right)f'''(\zeta)-f'^2(\zeta)+f(\zeta)f''(\zeta)-Kf'(\zeta)-Mf'(\zeta)=0.\\
\Rightarrow\ & \left(\frac{1+\beta}{\beta}\right)f'''(\zeta)+f(\zeta)f''(\zeta)-f'^2(\zeta)-(M+K)f'(\zeta)=0. \qquad (3.18)
\end{aligned}
$$

Now, for the conversion of energy equation (3.3), the following derivatives are required.

$$
\begin{aligned}
&\theta(\zeta)=\frac{T-T_\infty}{T_w-T_\infty},\\
&T=\theta(\zeta)(T_w-T_\infty)+T_\infty.\\
&\frac{\partial T}{\partial x}=0. \qquad (3.19)\\
&\frac{\partial T}{\partial y}=(T_w-T_\infty)\theta'(\zeta)\frac{\partial\zeta}{\partial y}\\
&\qquad=\left(\frac{a}{\nu}\right)^{\frac{1}{2}}(T_w-T_\infty)\theta'(\zeta). \qquad (3.20)\\
&\frac{\partial^2 T}{\partial y^2}=\left(\frac{a}{\nu}\right)^{\frac{1}{2}}(T_w-T_\infty)\theta''(\zeta)\frac{\partial\zeta}{\partial y}
\end{aligned}
$$

$$
\begin{aligned}
&= \left(\frac{a}{\nu}\right)^{\frac{1}{2}} (T_w - T_\infty)\theta''(\zeta) \left(\frac{a}{\nu}\right)^{\frac{1}{2}} \\
&= \left(\frac{a}{\nu}\right) (T_w - T_\infty)\theta''(\zeta). \qquad (3.21)
\end{aligned}
$$

$$
\begin{aligned}
\left(\frac{\partial T}{\partial y}\right)^2 &= \left(\left(\frac{a}{\nu}\right)^{\frac{1}{2}} (T_w - T_\infty)\theta'(\zeta)\right)^2 \\
&= \frac{a}{\nu}(T_w - T_\infty)^2\theta'^2(\zeta). \qquad (3.22)
\end{aligned}
$$

$$
\begin{aligned}
q_r &= -\frac{4\sigma^*}{3k^*}\frac{\partial T^4}{\partial y} \\
&= -\frac{4\sigma^*}{3k^*}\frac{\partial}{\partial y}(4T_\infty^3 T - 3T_\infty^4) \\
&= -\frac{4\sigma^*}{3k^*}\frac{\partial}{\partial y}(4T_\infty^3 T) \\
&= -\frac{16\sigma^*}{3k^*}T_\infty^3\frac{\partial T}{\partial y}.
\end{aligned}
$$

$$
\begin{aligned}
\frac{\partial q_r}{\partial y} &= -\frac{16\sigma^*}{3k^*}T_\infty^3\frac{\partial^2 T}{\partial y^2} \\
&= -\frac{16\sigma^*}{3k^*}T_\infty^3\left(\left(\frac{a}{\nu}\right)(T_w - T_\infty)\theta''(\zeta)\right). \qquad (3.23)
\end{aligned}
$$

$$
\frac{\partial C}{\partial y} = (C_w - C_\infty)\phi'(\zeta)\frac{\partial \zeta}{\partial y}. \qquad (3.24)
$$

$$
\frac{\partial C}{\partial y} = \left(\frac{a}{\nu}\right)^{\frac{1}{2}} (C_w - C_\infty)\phi'(\zeta). \qquad (3.25)
$$

Using (3.19) and (3.20) in the left hand side of (3.3),

$$
\begin{aligned}
u\frac{\partial T}{\partial x} + v\frac{\partial T}{\partial y} &= axf'(\zeta)(0) + \left(-(a\nu)^{\frac{1}{2}} f(\zeta)\right)\left(\left(\frac{a}{\nu}\right)^{\frac{1}{2}} (T_w - T_\infty)\theta'(\zeta)\right) \\
&= -(a\nu)^{\frac{1}{2}} f(\zeta)\left(\frac{a}{\nu}\right)^{\frac{1}{2}} (T_w - T_\infty)\theta'(\zeta) \\
&= -a(T_w - T_\infty)f(\zeta)\theta'(\zeta). \qquad (3.26)
\end{aligned}
$$

Using (3.21)-(3.25) in the right side of (3.3), we get

$$
\begin{aligned}
&\alpha\frac{\partial^2 T}{\partial y^2} + \tau\left(D_B\frac{\partial C}{\partial y}\frac{\partial T}{\partial y} + \frac{D_T}{T_\infty}\left(\frac{\partial T}{\partial y}\right)^2\right) - \frac{1}{(\rho Cp)}\frac{\partial q_r}{\partial y} \\
&= \alpha\left(\frac{a}{\nu}\right)(T_w - T_\infty)\theta''(\zeta) + \tau\Big[D_B\left(\frac{a}{\nu}\right)^{\frac{1}{2}}(T_w - T_\infty)\theta'(\zeta)\left(\frac{a}{\nu}\right)^{\frac{1}{2}}(C_w - C_\infty)\phi'(\zeta) \\
&\quad + \frac{D_T}{T_\infty}\left(\frac{a}{\nu}\right)(T_w - T_\infty)^2\theta'^2(\zeta)\Big] - \frac{1}{\rho c_p}\left(-\frac{16\sigma^* T_\infty^3}{3k^*}\left(\frac{a}{\nu}\right)(T_w - T_\infty)\theta''(\zeta)\right) \\
&= \alpha\left(\frac{a}{\nu}\right)(T_w - T_\infty)\theta''(\zeta) + \tau D_B\left(\frac{a}{\nu}\right)(T_w - T_\infty)\theta'(\zeta)(C_w - C_\infty)\phi'(\zeta)
\end{aligned}
$$

$$+\tau\frac{D_T}{T_\infty}\left(\frac{a}{\nu}\right)(T_w-T_\infty)^2\theta'^2(\zeta)+\frac{1}{\rho c_p}\left(\frac{16\sigma^*T_\infty^3}{3k^*}\left(\frac{a}{\nu}\right)(T_w-T_\infty)\theta''(\zeta)\right). \quad (3.27)$$

Comparing (3.26) and (3.27), the dimensionless form of (3.3), is obtained as follow.

$$\begin{aligned}
&-a(T_w-T_\infty)f(\zeta)\theta'(\zeta)=\tau D_B\left(\frac{a}{\nu}\right)(T_w-T_\infty)\theta'(\zeta)(C_w-C_\infty)\phi'(\zeta)\\
&\quad+\tau\frac{D_T}{T_\infty}\left(\frac{a}{\nu}\right)(T_w-T_\infty)^2\theta'^2(\zeta)+\frac{1}{\rho c_p}\left(\frac{16\sigma^*T_\infty^3}{3k^*}\left(\frac{a}{\nu}\right)(T_w-T_\infty)\theta''(\zeta)\right)\\
&\quad+\alpha\left(\frac{a}{\nu}\right)(T_w-T_\infty)\theta''(\zeta).\\
\Rightarrow\quad&-af(\zeta)\theta'(\zeta)=\alpha\left(\frac{a}{\nu}\right)\theta''(\zeta)+\tau D_B\left(\frac{a}{\nu}\right)\theta'(\zeta)(C_w-C_\infty)\phi'(\zeta)\\
&\quad+\tau\frac{D_T}{T_\infty}\left(\frac{a}{\nu}\right)(T_w-T_\infty)\theta'^2(\zeta)+\frac{1}{\rho c_p}\left(\frac{16\sigma^*T_\infty^3}{3k^*}\left(\frac{a}{\nu}\right)\theta''(\zeta)\right)\\
\Rightarrow\quad&\frac{a}{\nu}\left(\alpha+\frac{1}{\rho c_p}\frac{16\sigma^*T_\infty^3}{3k^*}\right)\theta''(\zeta)+af(\zeta)\theta'(\zeta)+\tau D_B\left(\frac{a}{\nu}\right)\theta'(\zeta)(C_w-C_\infty)\phi'(\zeta)\\
&\quad+\tau\frac{D_T}{T_\infty}\left(\frac{a}{\nu}\right)(T_w-T_\infty)\theta'^2(\zeta)=0\\
\Rightarrow\quad&\frac{a}{\nu}\left(\frac{k}{\rho c_p}+\frac{16\sigma^*T_\infty^3}{3k^*\rho c_p}\right)\theta''(\zeta)+af(\zeta)\theta'(\zeta)+\tau D_B\left(\frac{a}{\nu}\right)\theta'(\zeta)(C_w-C_\infty)\phi'(\zeta)\\
&\quad+\tau\frac{D_T}{T_\infty}\left(\frac{a}{\nu}\right)(T_w-T_\infty)\theta'^2(\zeta)=0\\
\Rightarrow\quad&\frac{a}{\nu}\frac{k}{\rho c_p}\left(1+\frac{16\sigma^*T_\infty^3}{3k^*k}\right)\theta''(\zeta)+af(\zeta)\theta'(\zeta)+\tau D_B\left(\frac{a}{\nu}\right)\theta'(\zeta)(C_w-C_\infty)\phi'(\zeta)\\
&\quad+\tau\frac{D_T}{T_\infty}\left(\frac{a}{\nu}\right)(T_w-T_\infty)\theta'^2(\zeta)=0\\
\Rightarrow\quad&\frac{\alpha}{\nu}\left(1+\frac{16\sigma^*T_\infty^3}{3k^*k}\right)\theta''(\zeta)+f(\zeta)\theta'(\zeta)+\frac{\tau D_B(C_w-C_\infty)}{\nu}\theta'(\zeta)\phi'(\zeta)\\
&\quad+\frac{\tau\ D_T(T_w-T_\infty)}{T_\infty\nu}\theta'^2(\zeta)=0\\
\Rightarrow\quad&\frac{1}{Pr}\left(1+\frac{4}{3}R\right)\theta''(\zeta)+f(\zeta)\theta'(\zeta)+Nb\theta'(\zeta)\phi'(\zeta)+Nt\theta'^2(\zeta)=0\\
\Rightarrow\quad&\frac{1}{Pr}\left(1+\frac{4}{3}R\right)\theta''(\zeta)+Nb\theta'(\zeta)\phi'(\zeta)+Nt\theta'^2(\zeta)+f(\zeta)\theta'(\zeta)=0. \qquad (3.28)
\end{aligned}$$

Now, we include below the procedure for the conversion of equation (3.4) into the dimensionless form.

$$\phi(\zeta)=\frac{C-C_\infty}{C_w-C_\infty},$$
$$C=(C_w-C_\infty)\phi(\zeta)+C_\infty.$$

$$\frac{\partial C}{\partial x} = 0. \tag{3.29}$$

$$\begin{aligned}\frac{\partial C}{\partial y} &= (C_w - C_\infty)\phi'(\zeta)\frac{\partial \zeta}{\partial y} \\ &= \left(\frac{a}{\nu}\right)^{\frac{1}{2}}(C_w - C_\infty)\phi'(\zeta).\end{aligned} \tag{3.30}$$

$$\begin{aligned}\frac{\partial^2 C}{\partial y^2} &= \left(\frac{a}{\nu}\right)^{\frac{1}{2}}(C_w - C_\infty)\phi''(\zeta)\frac{\partial \zeta}{\partial y} \\ &= \left(\frac{a}{\nu}\right)^{\frac{1}{2}}(C_w - C_\infty)\phi''(\zeta)\left(\frac{a}{\nu}\right)^{\frac{1}{2}} \\ &= \left(\frac{a}{\nu}\right)(C_w - C_\infty)\phi''(\zeta) \\ &= \left(\frac{a}{\nu}\right)(C_w - C_\infty)\phi''(\zeta).\end{aligned} \tag{3.31}$$

$$\frac{\partial^2 T}{\partial y^2} = \left(\frac{a}{\nu}\right)(T_w - T_\infty)\theta''(\zeta). \tag{3.32}$$

Using (3.29) and (3.30) in the left hand side of (3.4), we get:

$$\begin{aligned}u\frac{\partial C}{\partial x} + v\frac{\partial C}{\partial y} &= axf'(\zeta)(0) + \left(-(a\nu)^{\frac{1}{2}}f(\zeta)\right)\left(\left(\frac{a}{\nu}\right)^{\frac{1}{2}}(C_w - C_\infty)\phi'(\zeta)\right) \\ &= -(a\nu)^{\frac{1}{2}}f(\zeta)\left(\frac{a}{\nu}\right)^{\frac{1}{2}}(C_w - C_\infty)\phi'(\zeta) \\ &= -a(C_w - C_\infty)f(\zeta)\phi'(\zeta).\end{aligned} \tag{3.33}$$

Using (3.31) and (3.32) in the right hand side of (3.4), the following is acheived:

$$D_B\frac{\partial^2 C}{\partial y^2} + \frac{D_T}{T_\infty}\frac{\partial^2 T}{\partial y^2} = D_B\left(\frac{a}{\nu}\right)(C_w - C_\infty)\phi''(\zeta) + \frac{D_T}{T_\infty}\left(\frac{a}{\nu}\right)(T_w - T_\infty)\theta''(\zeta). \tag{3.34}$$

Comparing (3.33) and (3.34),

$$\begin{aligned}& -a(C_w - C_\infty)f(\zeta)\phi'(\zeta) = D_B\left(\frac{a}{\nu}\right)(C_w - C_\infty)\phi'' + \frac{D_T}{T_\infty}\left(\frac{a}{\nu}\right)(T_w - T_\infty)\theta''(\zeta). \\ \Rightarrow\quad & -\frac{\nu}{D_B}f(\zeta)\phi'(\zeta) = \phi''(\zeta) + \frac{D_T(T_w - T_\infty)}{T_\infty D_B(C_w - C_\infty)}\theta''(\zeta). \\ \Rightarrow\quad & -Scf(\zeta)\phi'(\zeta) = \phi''(\zeta) + \frac{\tau\nu D_T(T_w - T_\infty)}{\tau\nu T_\infty D_B(C_w - C_\infty)}\theta''(\zeta). \\ \Rightarrow\quad & \phi''(\zeta) + Scf(\zeta)\phi'(\zeta) + \frac{D_T\tau(T_w - T_\infty)\nu}{T_\infty\nu D_B\tau(C_w - C_\infty)}\theta''(\zeta) = 0. \\ \Rightarrow\quad & \phi''(\zeta) + Scf(\zeta)\phi'(\zeta) + \frac{Nt}{Nb}\theta''(\zeta) = 0.\end{aligned} \tag{3.35}$$

The corresponding BCs are transformed into the non-dimensional form through the following procedure.

$$
\begin{aligned}
& u = U_w(x) = ax, && at \quad y = 0. \\
\Rightarrow \quad & u = axf'(\zeta), && at \quad \zeta = 0. \\
\Rightarrow \quad & axf'(\zeta) = ax, && at \quad \zeta = 0. \\
\Rightarrow \quad & f'(\zeta) = 1, && at \quad \zeta = 0. \\
\Rightarrow \quad & f'(0) = 1. && \\
& v = 0, && at \quad y = 0. \\
\Rightarrow \quad & -(a\nu)^{\frac{1}{2}} f(0) = 0, && at \quad \zeta = 0. \\
\Rightarrow \quad & f(0) = 0. && \\
& T = T_w, && at \quad y = 0. \\
\Rightarrow \quad & \theta(\zeta)(T_w - T_\infty) + T_\infty = T_w, && at \quad \zeta = 0. \\
\Rightarrow \quad & \theta(\zeta)(T_w - T_\infty) = (T_w - T_\infty), && at \quad \zeta = 0. \\
\Rightarrow \quad & \theta(\zeta) = 1, && at \quad \zeta = 0. \\
\Rightarrow \quad & \theta(0) = 1. && \\
& C = C_w, && at \quad y = 0. \\
\Rightarrow \quad & \phi(\zeta)(C_w - C_\infty) + C_\infty = C_w, && at \quad \zeta = 0. \\
\Rightarrow \quad & \phi(\zeta)(C_w - C_\infty) = (C_w - C_\infty), && at \quad \zeta = 0. \\
\Rightarrow \quad & \phi(\zeta) = 1, && at \quad \zeta = 0. \\
\Rightarrow \quad & \phi(0) = 1. && \\
& u \to (0), && as \quad y \to \infty. \\
\Rightarrow \quad & af'(\zeta)x \to (0), && as \quad y \to \infty. \\
\Rightarrow \quad & axf'(\zeta) \to (0), && \\
\Rightarrow \quad & f'(\zeta) \to (0), && as \quad \zeta \to \infty. \\
\Rightarrow \quad & f'(\infty) \to 0. && \\
& T \to T_\infty, && as \quad y \to \infty. \\
\Rightarrow \quad & \theta(\zeta)(T_w - T_\infty) + T_\infty \to T_\infty, && \\
\Rightarrow \quad & \theta(\zeta)(T_w - T_\infty) \to 0, && as \quad \zeta \to \infty.
\end{aligned}
$$

$$\begin{aligned}
&\Rightarrow \quad \theta(\zeta) \to 0, && as \quad \zeta \to \infty.\\
&\Rightarrow \quad \theta(\infty) \to 0.\\
&\quad\quad C \to C_\infty, && as \quad y \to \infty.\\
&\Rightarrow \quad \phi(\zeta)(C_w - C_\infty) + C_\infty \to C_\infty,\\
&\Rightarrow \quad \phi(\zeta)(C_w - C_\infty) \to 0,\\
&\Rightarrow \quad \phi(\zeta) \to 0, && as \quad \zeta \to \infty.\\
&\Rightarrow \quad \phi(\infty) \to 0.
\end{aligned}$$

The final dimensionless form of the governing model, is

$$\left(\frac{1+\beta}{\beta}\right) f'''(\zeta) + f(\zeta)f''(\zeta) - f'^2(\zeta) - (M+K)f'(\zeta) = 0, \tag{3.36}$$

$$\frac{1}{Pr}\left(1 + \frac{4}{3}R\right)\theta''(\zeta) + Nb\theta'(\zeta)\phi'(\zeta) + Nt\theta'^2(\zeta) + f(\zeta)\theta'(\zeta) = 0, \tag{3.37}$$

$$\phi''(\zeta) + Scf(\zeta)\phi'(\zeta) + \frac{Nt}{Nb}\theta''(\zeta) = 0. \tag{3.38}$$

The associated BCs (3.5) in the dimensionless form are:

$$\left.\begin{aligned}
&f(0) = 0, \quad f'(0) = 1, \quad \theta(0) = 1, \quad \phi(0) = 1,\\
&f'(\infty) \to 0, \quad \theta(\infty) \to 0 \quad and \quad \phi(\infty) \to 0.
\end{aligned}\right\} \tag{3.39}$$

Different dimensionless parameters used in equations (3.36)-(3.38) are formulated as follows.

$$\begin{aligned}
&M = \frac{\sigma B_0^2}{\rho a}, \quad R = \frac{4\sigma^* T_\infty^3}{kk^*}, \quad Nb = \frac{\tau D_B(C_w - C_\infty)}{\nu},\\
&Pr = \frac{\nu}{\alpha}, \quad Sc = \frac{\nu}{D_B}, \quad K = \frac{\nu}{k_1 a}, \quad Nt = \frac{\tau D_T(T_w - T_\infty)}{T_\infty \nu}.
\end{aligned}$$

The skin friction coefficient, is defined as:

$$C_f = \frac{\tau_w\big|_{y=0}}{\rho U_w^2}. \tag{3.40}$$

To achieve the dimensionless form of skin friction coefficient C_f the following steps will be helpful.

Since

$$\tau_w = \mu\left(\frac{\partial u}{\partial y}\right)_{y=0}, \tag{3.41}$$

$$\begin{aligned}
C_f &= \frac{1}{\rho U_w^2}\mu\left(\frac{\partial u}{\partial y}\right)_{y=0} \\
&= \frac{1}{\rho a^2 x^2}\mu\left(axf''(\zeta)\left(\frac{a}{\nu}\right)^{\frac{1}{2}}\right) \\
&= \frac{\rho\nu}{\rho a^2 x^2}\left(axf''(\zeta)\left(\frac{a}{\nu}\right)^{\frac{1}{2}}\right) \\
&= \frac{\nu a^{\frac{3}{2}} x}{a^2 x^2 \nu^{\frac{1}{2}}} f''(\zeta) \\
&= \frac{\nu^{\frac{2}{2}}}{a x^{\frac{2}{2}}} f''(\zeta) \\
&= Re_x^{\frac{-1}{2}} f''(\zeta) \\
&= \frac{1}{Re_x^{\frac{1}{2}}} f''(\zeta).
\end{aligned}$$

$$\Rightarrow \quad Re_x^{\frac{1}{2}} C_f = f''(\zeta), \tag{3.42}$$

where Re stands for the Reynolds number, which is defined as $Re = \frac{xu_x(x)}{\nu_f}$.

The local Nusselt number is formulated as:

$$Nu_x = \frac{xq_w}{k(T_w - T_\infty)}. \tag{3.43}$$

To achieve the dimensionless form of local Nusselt number Nu_x, the following steps will be helpful.

Since

$$q_w = -k\left(\frac{\partial T}{\partial y}\right)_{y=0}, \tag{3.44}$$

$$\begin{aligned}
Nu_x &= \frac{-xk}{k(T_w - T_\infty)}\left(\frac{\partial T}{\partial y}\right)_{y=0}, \\
&= \frac{-x}{(T_w - T_\infty)}\left(\left(\frac{a}{\nu}\right)^{\frac{1}{2}}(T_w - T_\infty)\theta'(\zeta)\right)
\end{aligned}$$

$$
\begin{aligned}
&= -\frac{xa^{\frac{1}{2}}}{\nu^{\frac{1}{2}}}\theta'(\zeta) \\
&= -Re_x^{\frac{1}{2}}\theta'(\zeta). \\
\Rightarrow \quad \frac{Nu_x}{Re_x^{\frac{1}{2}}} &= -\theta'(\zeta).
\end{aligned} \tag{3.45}
$$

The local Sherwood number is defined as:

$$
Sh_x = \frac{xq_m}{D_B(C_w - C_\infty)}. \tag{3.46}
$$

To the dimensionless form of Sh_x, the following steps will be helpful.

Since

$$
q_m = -D_B\left(\frac{\partial C}{\partial y}\right)_{y=0}, \tag{3.47}
$$

$$
\begin{aligned}
Sh_x &= -\frac{xD_B}{D_B(C_w - C_\infty)}\left(\frac{\partial C}{\partial y}\right)_{y=0} \\
&= -\frac{x}{(C_w - C_\infty)}\left(\frac{a}{\nu}\right)^{\frac{1}{2}}(C_w - C_\infty)\phi'(\zeta) \\
&= -\frac{x}{(C_w - C_\infty)}\left(\left(\frac{a}{\nu}\right)^{\frac{1}{2}}(C_w - C_\infty)\phi'(\zeta)\right) \\
&= -x\left(\frac{a}{\nu}\right)^{\frac{1}{2}}\phi'(\zeta) \\
&= -\frac{xa^{\frac{1}{2}}}{\nu^{\frac{1}{2}}}\phi'(\zeta) \\
&= -Re_x^{\frac{1}{2}}\phi'(\zeta) \\
\Rightarrow \quad \frac{Sh_x}{Re_x^{\frac{-1}{2}}} &= -\phi'(\zeta).
\end{aligned} \tag{3.48}
$$

3.3 Numerical Method for Solution

The shooting method has been used to solve the system of ordinary differential equations (3.36)-(3.38). The following notations have been considered.

$$
f = Z_1, \qquad f' = Z_1' = Z_2, \qquad f'' = Z_1'' = Z_2' = Z_3, \qquad f''' = Z_3'.
$$

The following system of first order ODEs is created by converting the momentum equation.

$$
\begin{aligned}
&Z_1' = Z_2, && Z_1(0) = 0.\\
&Z_2' = Z_3, && Z_2(0) = 1.\\
&Z_3' = \left(\frac{\beta}{1+\beta}\right)\left(-Z_1Z_3 + Z_2^2 + (M+K)Z_2\right), && Z_3(0) = p.
\end{aligned}
$$

The RK-4 method will be used to numerically solve the above mentioned initial value problem. The bounded domain $[0,\ \zeta_\infty]$ has been used in place of the unbounded domain $[0\ ,\ \infty)$ for the numerical results with the observation that it produces an asymptotic covergence of the solution. The missing condition p is selected so that the subsequent relation is met.

$$
Z_2(\zeta_\infty, p) = 0.
$$

Newton's method will be used to find p. This method has the following iterative scheme.

$$
p^{(n+1)} = p^{(n)} - \frac{Z_2(\zeta_\infty, p^{(n)})}{\left(\frac{\partial}{\partial p}(Z_2(\zeta_\infty, p))\right)^{(n)}}.
$$

We further introduce the following notations:

$$
\frac{\partial Z_1}{\partial p} = Z_4, \qquad \frac{\partial Z_2}{\partial p} = Z_5, \qquad \frac{\partial Z_3}{\partial p} = Z_6.
$$

As a result of these new notations, the Newton's iterative scheme gets the form:

$$
p^{(n+1)} = p^{(n)} - \frac{Z_2(\zeta_\infty, p^{(n)})}{Z_5(\zeta_\infty, p^{(n)})}.
$$

Now differentiating the system of three first order ODEs with respect to p, we get another system of ODEs, as follows.

$$
Z_4' = Z_5, \qquad\qquad Z_4(0) = 0.
$$

$$
\begin{aligned}
Z_5' &= Z_6, & Z_5(0) &= 0.\\
Z_6' &= \left(\frac{\beta}{1+\beta}\right)\left(-Z_4Z_3 - Z_1Z_6 + 2Z_2Z_5 + (M+K)Z_5\right), & Z_6(0) &= 1.
\end{aligned}
$$

The stopping criteria for the Newton's technique is set as.

$$| Z_2(\zeta_\infty, p) | < \epsilon,$$

where $\epsilon > 0$ is an arbitrarily small positive number. From now onward ϵ has been taken as 10^{-10}.

Now, to solve equations (3.37) and (3.38) numerically by using shooting method, assume f as a known function. The notations below are used for the implementation of the shooting method.

$$\theta = Y_1, \quad \theta' = Y_2, \quad \theta'' = Y_2', \quad \phi = Y_3, \quad \phi' = Y_4, \quad \phi'' = Y_4', \quad A_1 = \left(1 + \frac{4}{3}R\right).$$

The system of equations (3.37) and (3.38), can be written in the form of the following first order coupled ODEs.

$$
\begin{aligned}
Y_1' &= Y_2, & Y_1(0) &= 1.\\
Y_2' &= -\frac{Pr}{A_1}\Big[NbY_2Y_4 + NtY_2^2 + fY_2\Big], & Y_2(0) &= l.\\
Y_3' &= Y_4, & Y_3(0) &= 1.\\
Y_4' &= -ScfY_4 + \frac{Nt}{Nb}\left[\frac{Pr}{A_1}\Big[NbY_2Y_4 + NtY_2^2 + fY_2\Big]\right], & Y_4(0) &= m.
\end{aligned}
$$

The RK-4 technique will be used to numerically solve the initial value problem mentioned above. The missing conditions l and m in the above system of equations must be selected in such a way.

$$Y_1(\zeta_\infty, l, m) = 0, \qquad Y_3(\zeta_\infty, l, m) = 0.$$

To solve the above algebaric equations, we apply the Newton's method which has the following scheme.

$$\begin{bmatrix} l \\ m \end{bmatrix}^{(n+1)} = \begin{bmatrix} l \\ m \end{bmatrix}^{(n)} - \left(\begin{bmatrix} \frac{\partial Y_1}{\partial l} & \frac{\partial Y_1}{\partial m} \\ \frac{\partial Y_3}{\partial l} & \frac{\partial Y_3}{\partial m} \end{bmatrix}^{-1} \begin{bmatrix} Y_1 \\ Y_3 \end{bmatrix} \right)^{(n)}$$

Now, introduce the following notations,

$$\frac{\partial Y_1}{\partial l} = Y_5, \qquad \frac{\partial Y_2}{\partial l} = Y_6, \qquad \frac{\partial Y_3}{\partial l} = Y_7, \qquad \frac{\partial Y_4}{\partial l} = Y_8.$$
$$\frac{\partial Y_1}{\partial m} = Y_9, \qquad \frac{\partial Y_2}{\partial m} = Y_{10}, \qquad \frac{\partial Y_3}{\partial m} = Y_{11}, \qquad \frac{\partial Y_4}{\partial m} = Y_{12}.$$

As the result of these new notations, the Newton's iterative scheme gets the form.

$$\begin{bmatrix} l \\ m \end{bmatrix}^{(n+1)} = \begin{bmatrix} l \\ m \end{bmatrix}^{(n)} - \left(\begin{bmatrix} Y_5 & Y_9 \\ Y_7 & Y_{11} \end{bmatrix}^{-1} \begin{bmatrix} Y_1 \\ Y_3 \end{bmatrix} \right)^{(n)}$$

Now differentiating the system of four first order ODEs with respect to l, and m we get another system of ODEs, as follows.

$$
\begin{aligned}
&Y_5' = Y_6, && Y_5(0) = 0.\\
&Y_6' = -\frac{Pr}{A_1}\Big[Nb(Y_6Y_4 + Y_2Y_8) + 2NtY_2Y_6 + fY_6\Big] && Y_6(0) = 1.\\
&Y_7' = Y_8, && Y_7(0) = 0.\\
&Y_8' = -ScfY_8 + \frac{Nt}{Nb}\left[\frac{Pr}{A_1}\Big[Nb(Y_6Y_4 + Y_2Y_8) + 2NtY_2Y_6 + fY_6\Big]\right], && Y_8(0) = 0.\\
&Y_9' = Y_{10}, && Y_9(0) = 0.\\
&Y_{10}' = -\frac{Pr}{A_1}\Big[Nb(Y_{10}Y_4 + Y_2Y_{12}) + 2NtY_2Y_{10} + fY_{10}\Big], && Y_{10}(0) = 0.\\
&Y_{11}' = Y_{12}, && Y_{11}(0) = 0.\\
&Y_{12}' = -ScfY_{12} + \frac{Nt}{Nb}\left[\frac{Pr}{A_1}\Big[Nb(Y_{10}Y_4 + Y_2Y_{12}) + 2NtY_2Y_{10} + fY_{10}\Big]\right], && Y_{12}(0) = 1.
\end{aligned}
$$

The stopping criteria for the Newton's method is set as.

$$max\{|Y_1(\zeta_\infty, l, m)|, |Y_3(\zeta_\infty, l, m)|\} < \epsilon.$$

3.4 Representation of Graphs and Tables

A thorough discussion on the graphs and tables has been conducted which contains the impact of dimensionless parameters on the skin friction coefficient $(Re_x)^{\frac{1}{2}}C_f$, local Nusselt number $(Re_x)^{-\frac{1}{2}}Nu_x$ and local Sherwood number $(Re_x)^{-\frac{1}{2}}Sh_x$. Table 3.1 explains the impact of magnetic parameter M and Casson fluid parameter β on $(Re_x)^{\frac{1}{2}}C_f$. For the rising values of M, the skin fraction coefficient $(Re_x)^{\frac{1}{2}}C_f$ increases. Table 3.1 shows the interval I_f where from the missing condition can be chosen. It is remarkable that the interval mentioned offers a considerable flexibility for the choice of the initial guess.

In Table 3.2, the effect of significant parameters on local Nusselt number $(Re_x)^{-\frac{1}{2}}Nu_x$ and local Sherwood number $(Re_x)^{-\frac{1}{2}}Sh_x$ has been discussed. The rising pattern is found in $(Re_x)^{-\frac{1}{2}}Sh_x$ and decreasing behavior noticed in $(Re_x)^{-\frac{1}{2}}Nu_x$ due to increasing values of R. Table 3.2 the missing initial conditions $\theta(\zeta)$ and $\phi(\zeta)$ can be chosen from $[I_g, I_h]$. It is remarkable that the interval mentioned offers a considerable flexibility for the choice of the initial guess.

Figures 3.2 and 3.3 show the impact of Casson fluid parameter β on the velocity profile $f'(\zeta)$ and temperature profile $\theta(\zeta)$. By increasing the value of β, the velocity of the fluid decreases and the temperature increases. When Casson fluid parameter β is incresed, the yield stress is decreased and Casson acts like Newtonain fluid. Furthermore, it is inferred that the velocity of Casson fluid exceeds that of the Newtonian fluid.

Figure 3.4 displays the impact of M on the velocity distribution. By rising the values of M, the velocity distribution shows a decreasing behavior due to the presence of the Lorentz force. Figure 3.5 describes the impact of M on the temperature distribution. The temperature distribution expands by rising the values of the M. Figures 3.6 and 3.7 indicate the impact of Nb on the dimensionless temperature

$\theta(\zeta)$ and concentration distribution $\phi(\zeta)$. The behavior of temperature distribution is increased and concentration profile is decreased due to the accelerating values of Nb. Figures 3.8 and 3.9 illustrate the impact of Nt on $\theta(\zeta)$ and $\phi(\zeta)$. By taking bigger values of Nt into account, both the temperature and concentration distributions increase. Furthermore, a growth in the related thermal and concentration boundary layer has been observed. Figure 3.10 represents the impact of thermal radiation R on the temperature profile $\theta(\zeta)$. In this graph, it is observed that on the rising values of R, the temperature profile $\theta(\zeta)$ also increases. So, the rate of heat transfer decreases with an increase in the thermal radiation R, because of which the temperature profile $\theta(\zeta)$ increases.

The effect of magnetic parameter and the Casson nanofluid on the local Nusselt number and skin friction coefficient, respectively, is illustrated in Figures 3.11 and 3.12. Temperature gradients will be higher when the Casson parameter's value is bigger. However, if the magnetic force increases, the thickness of the boundary layer will also decrease. Figure 3.12 illustrates how the skin friction coefficient reduces when the Casson parameter the and magnetic parameter values increase. Figure 3.13 illustrates the effect of Nt and Nb on the local Nusselt number. As the values of Nb and Nt are increased, it is clear that the dimensionless temperature rate drops continuously. Figure 3.14 indicates the impact of Prandlt number and radiation parameter on the temperature gradient. The local Nusselt number rises along with an increase in the values of Pr. As the radiation parameter rises, the heat transfer rate declines.

TABLE 3.1: Results of $(Re_x)^{\frac{1}{2}}C_f$ for various parameters

M	β	K	$(Re_x)^{\frac{1}{2}}C_f$	I_f
0.1	0.5	0.3	-0.6831	[-0.7, 0.6]
0.2			-0.7071	[-0.7, 0.1]
0.5			-0.7746	[-0.7, 0.2]
	1.0	0.3	-0.9486	[-0.9, -0.4]
	1.5		-1.0392	[-1.1, -0.6]
	2.0		-1.0954	[-1.1, -0.8]

TABLE 3.2: Results of $-(Re_x)^{-\frac{1}{2}}Nu_x$ and $-(Re_x)^{-\frac{1}{2}}Sh_x$ with some fixed parameters $Pr = 7.0$, $K = 0.3$, $Sc = 0.1$.

M	R	β	Nb	Nt	$-(Re_x)^{-\frac{1}{2}}Nu_x$	$-(Re_x)^{-\frac{1}{2}}Sh_x$	I_g	I_h
0.2	0.25	0.5	0.1	0.1	1.564456	-1.236102	[-2.0, 2.0]	[-2.0, 3.0]
0.3					1.560033	-1.233961	[-2.0, 1.0]	[-2.0, 4.0]
0.5					1.551488	-1.229542	[-2.5, 2.0]	[-2.0, 1.5]
0.2	1.0				1.165690	-0.844370	[-2.0, 2.5]	[-2.0, 1.0]
	2.0				0.908916	-0.593840	[-2.0, 2.0]	[-2.0, 3.0]
	4.0				0.661957	-0.354479	[-2.0, 3.0]	[-2.0, 1.0]
		1.5			1.516893	-1.208542	[-2.0, 2.5]	[-2.0, 1.0]
		2.0			1.506442	-1.201414	[-3.0, 2.0]	[-2.0, 2.0]
		0.5	0.2		1.502551	-0.499103	[-2.0, 3.5]	[-1.5, 3.0]
			0.4		1.389757	-0.131341	[-2.0, 6.0]	[-1.0, 5.0]
			0.1	0.2	1.512651	-2.548789	[-2.0, 3.0]	[-3.0, 3.0]
				0.3	1.461821	-3.761786	[-3.0, 3.0]	[-3.0, 3.0]
				0.4	1.411979	-4.878093	[-2.5, 2.5]	[-2.0, 1.5]

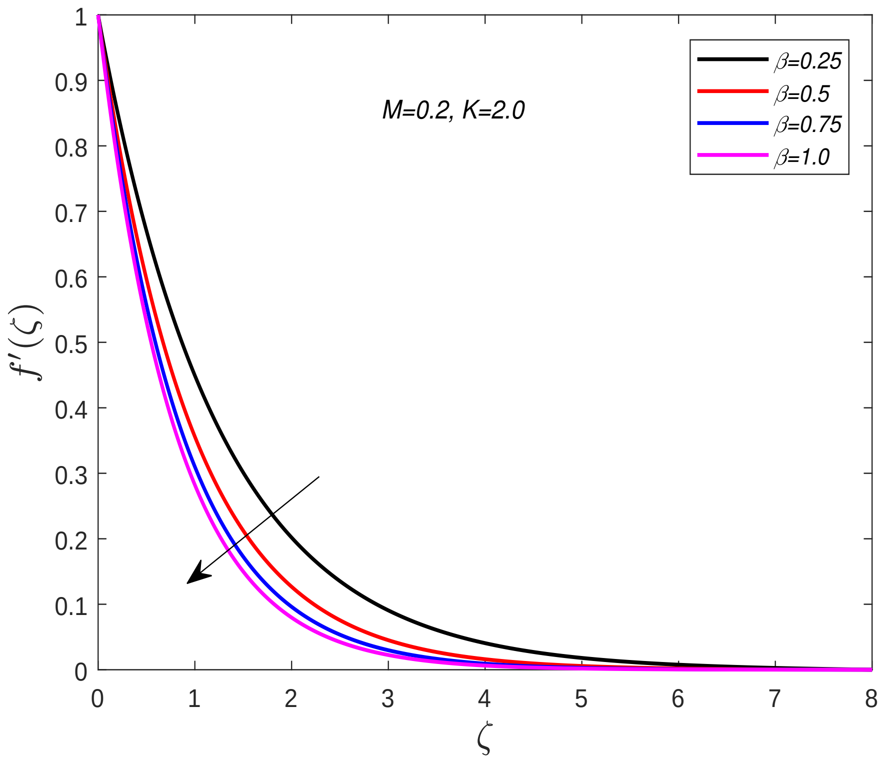

FIGURE 3.2: Velocity profile $f'(\zeta)$ due to change in β.

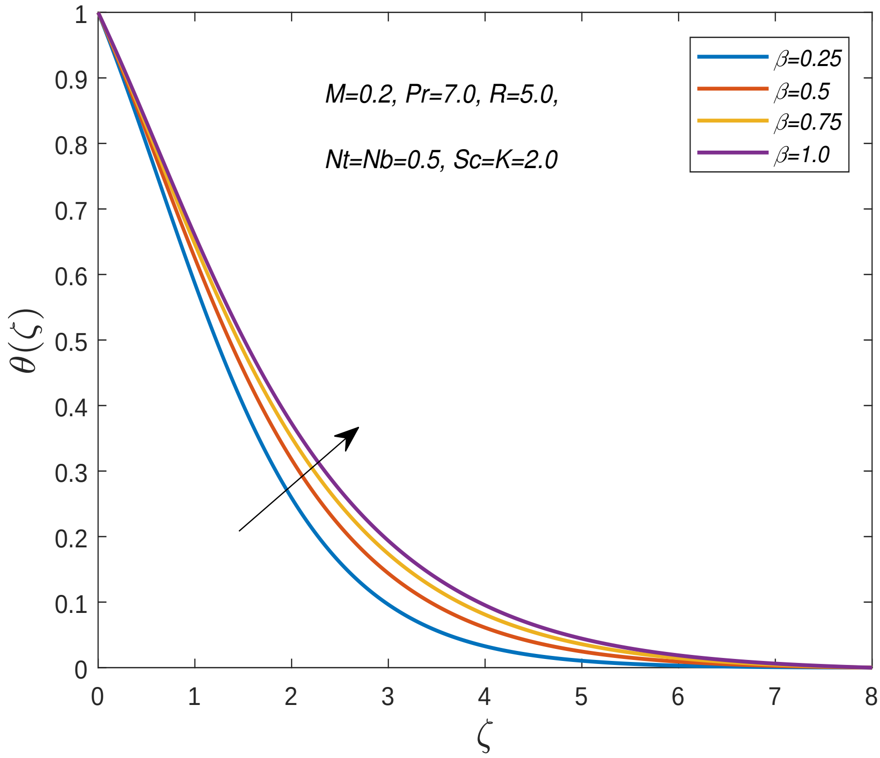

FIGURE 3.3: Temperature profile $\theta(\zeta)$ due to change in β.

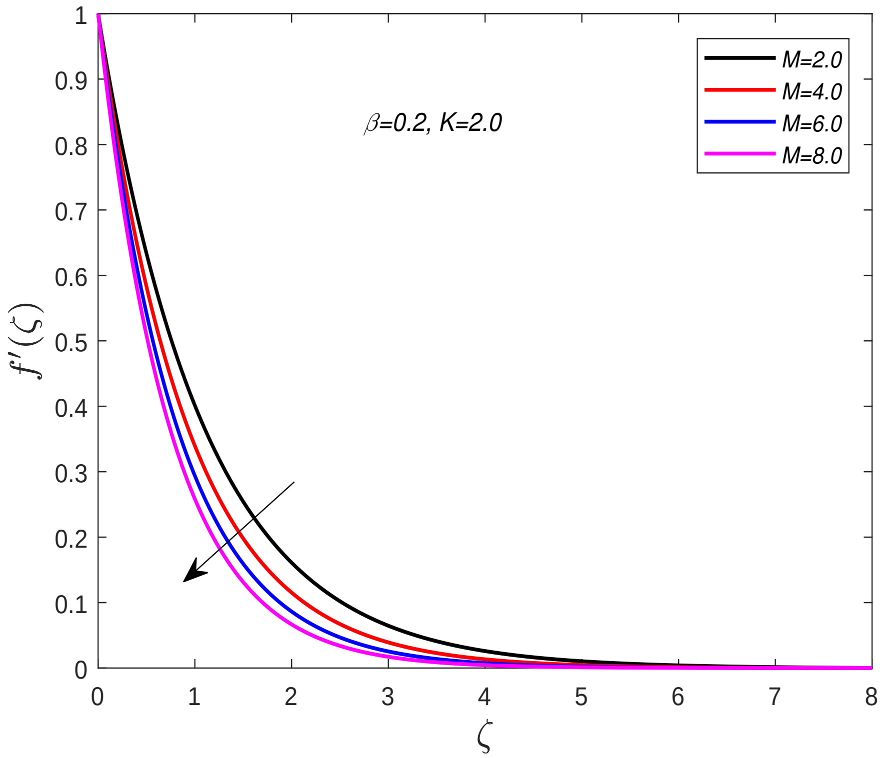

FIGURE 3.4: Velocity profile $f'(\zeta)$ due to change in M.

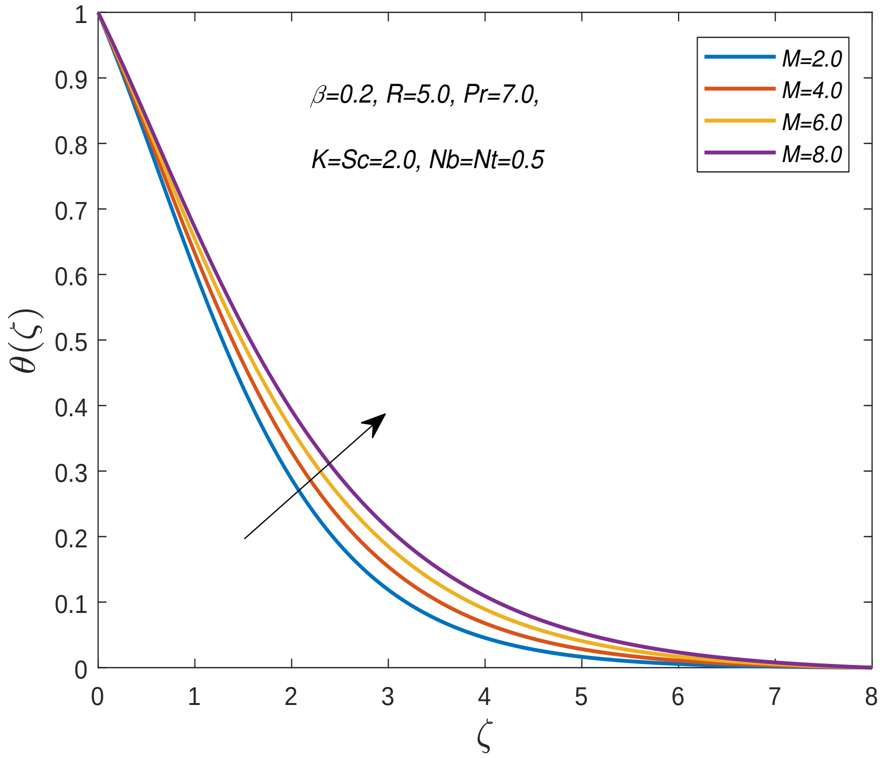

FIGURE 3.5: Temperature profile $\theta(\zeta)$ due to change in M.

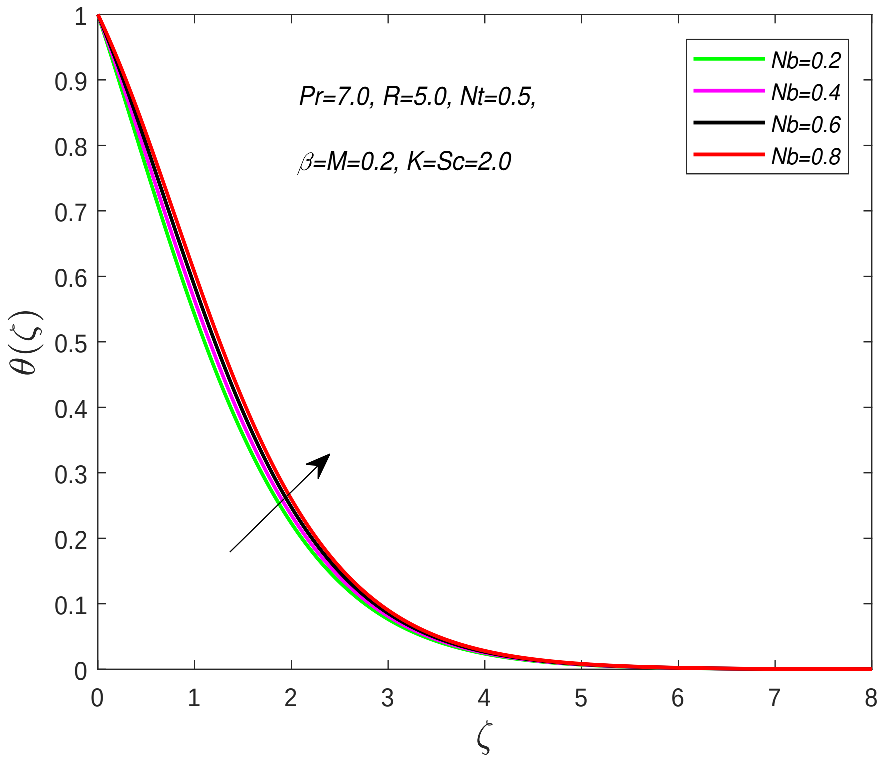

FIGURE 3.6: Temperature profile $\theta(\zeta)$ due to change in Nb.

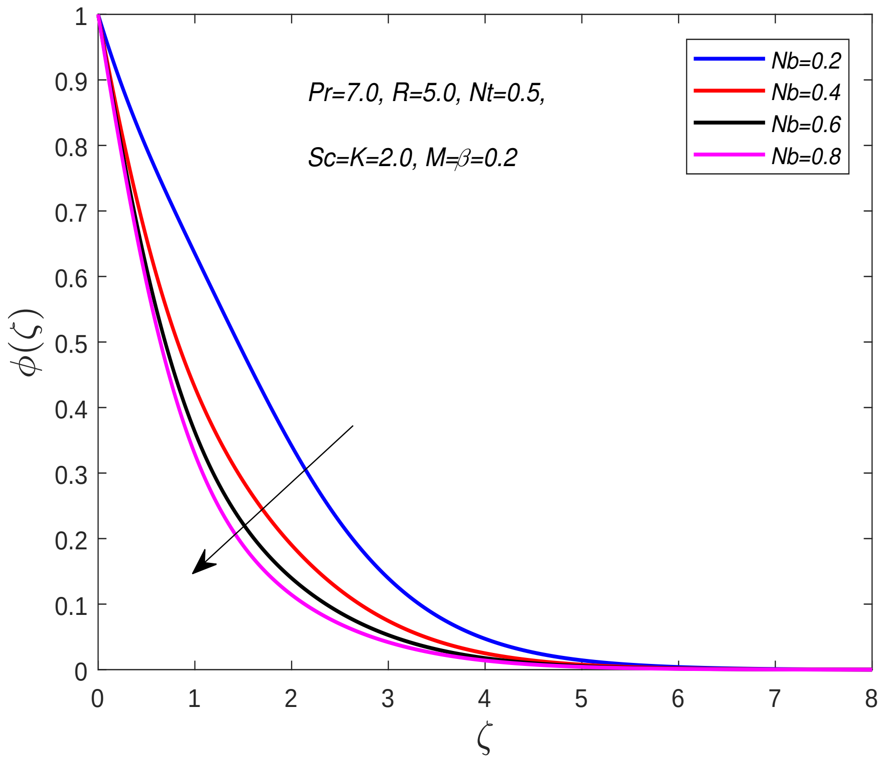

FIGURE 3.7: Concentration profile $\phi(\zeta)$ due to change in Nb.

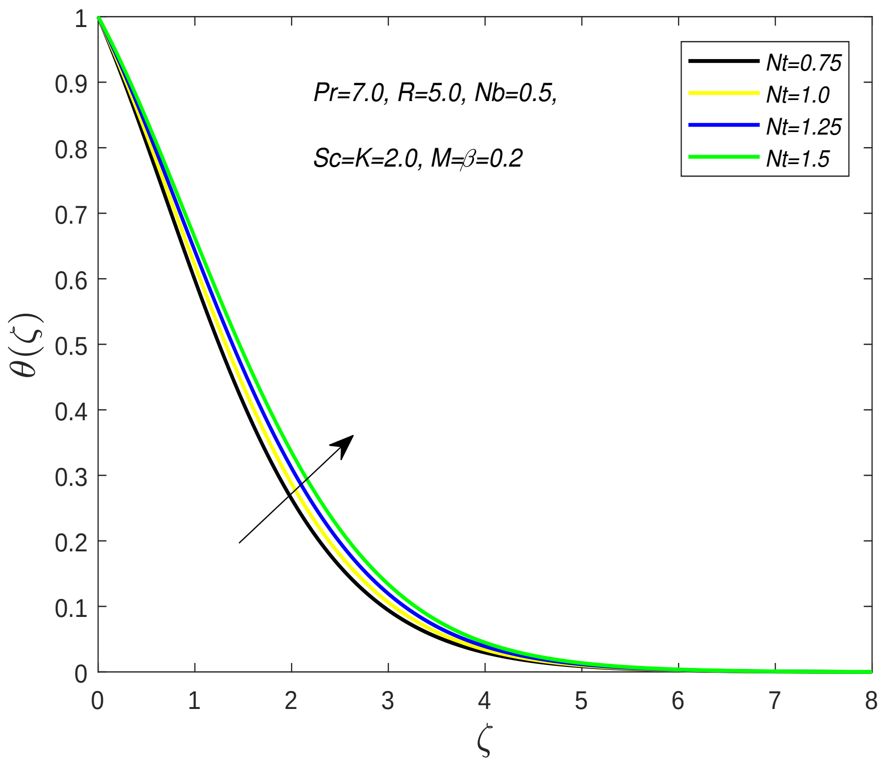

FIGURE 3.8: Temperature profile $\theta(\zeta)$ due to change in Nt.

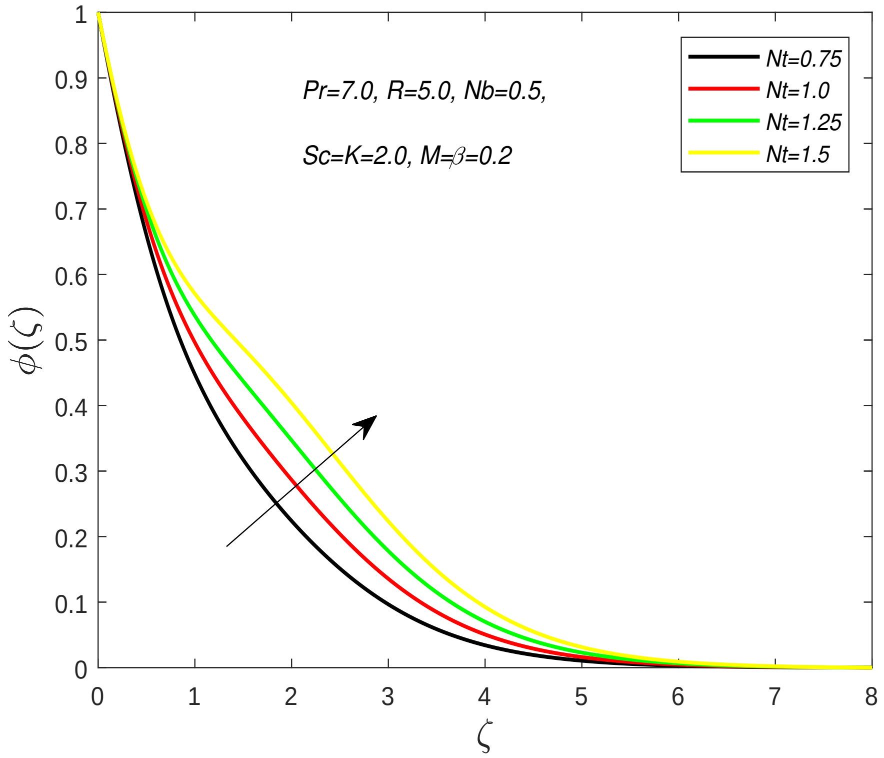

Figure 3.9: Concentration profile $\phi(\zeta)$ due to change in Nt.

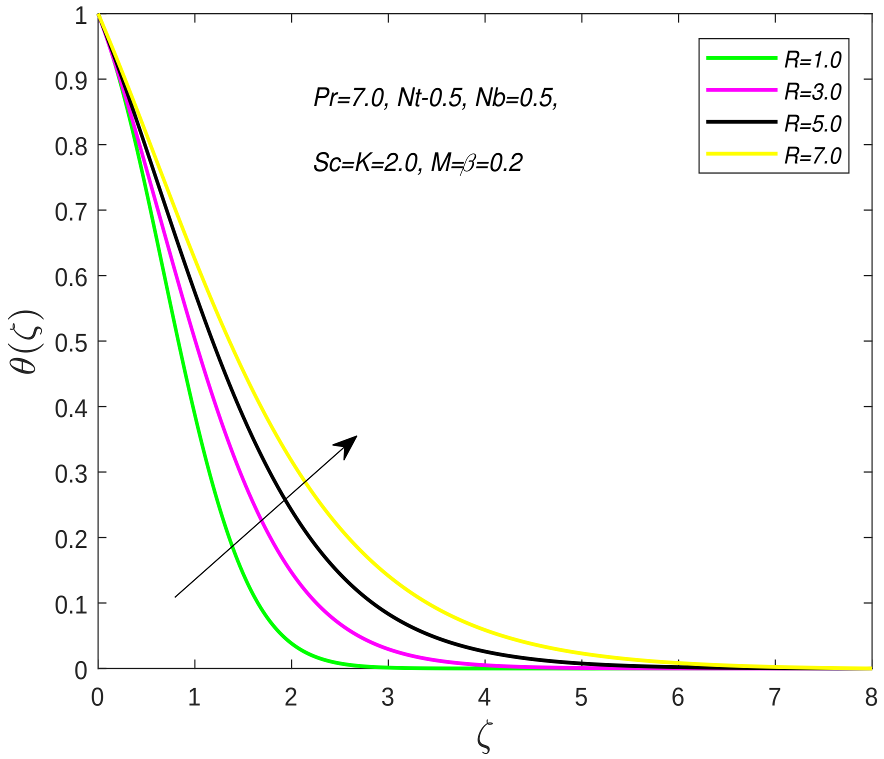

Figure 3.10: Temperature profile $\theta(\zeta)$ due to change in R.

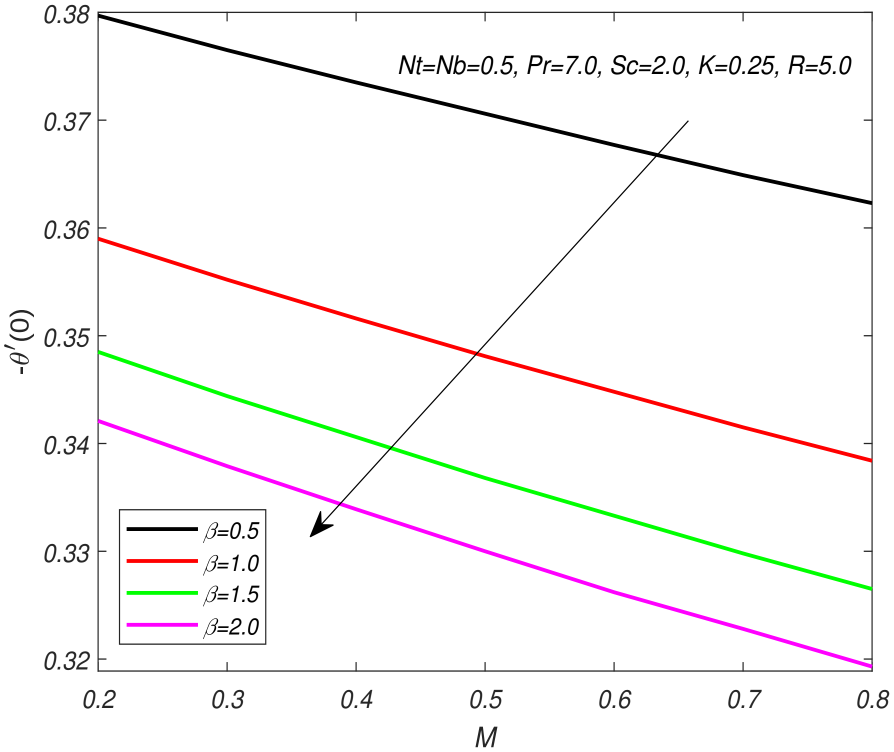

FIGURE 3.11: Impact of β and M on the temperature gradient.

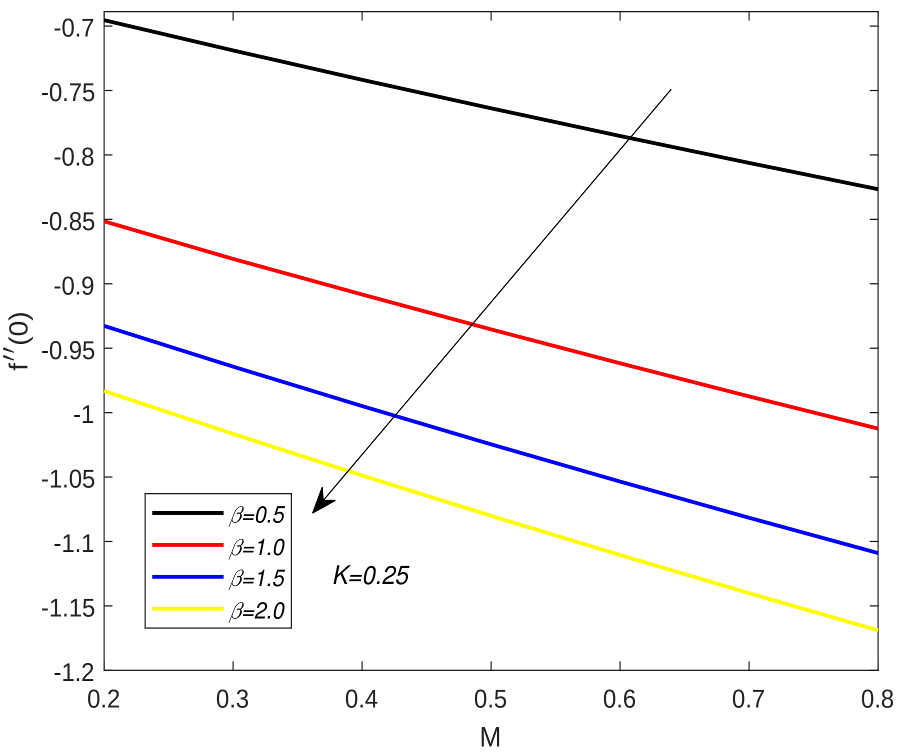

FIGURE 3.12: Impact of β and M on the skin friction coefficient.

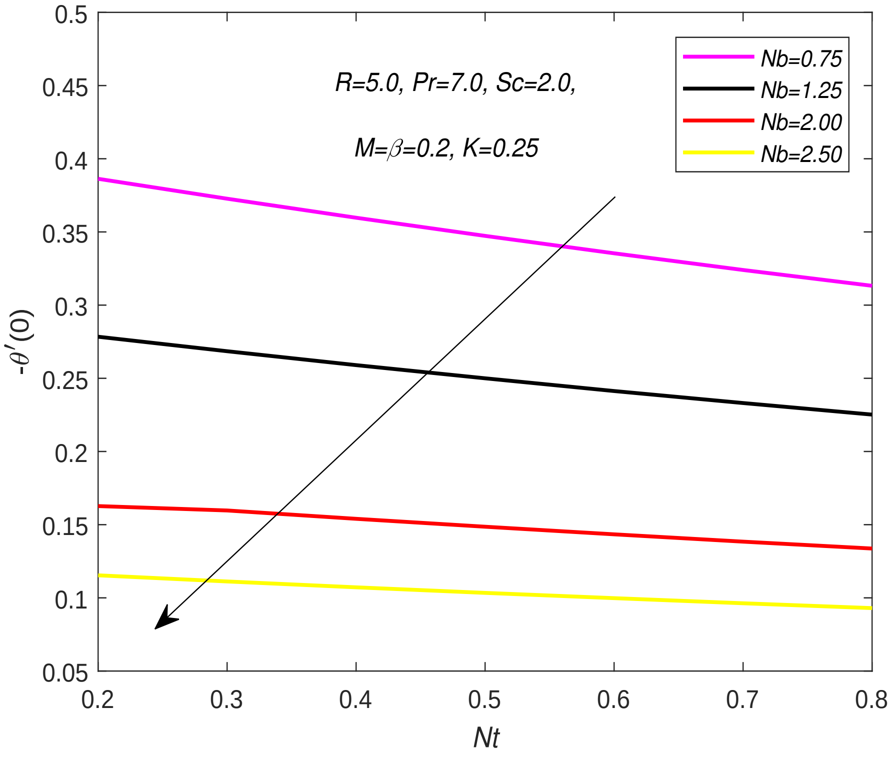

FIGURE 3.13: Impact of Nb and Nt on the temperature gradient.

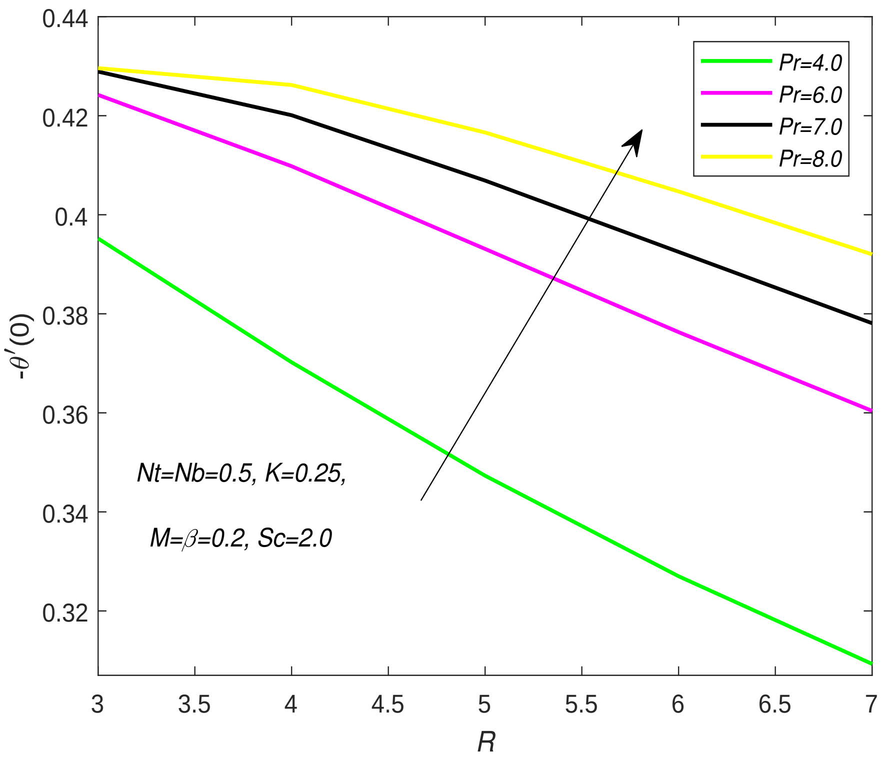

FIGURE 3.14: Impact of Pr and R on the temperature gradient.

Chapter 4

MHD Casson Nanofluid Flow with Cattaneo-Christov Heat Flux and Mass Transfer over a Stretching Sheet

4.1 Introduction

This chapter contains an extension of the model [49] discussed in Chapter 3 by considering Cattaneo-Christov heat flux in the temperature equation. Furthermore, chemical reaction, is also included in the concentration equation. The governing nonlinear PDEs are converted into a system of dimensionless ODEs by utilizing the appropriate transformations. The numerical solution of ODEs is obtaind by applying numerical method known as shooting method. At the end of this chapter, the final results are discussed for significant parameters affecting velocity proflie $f'(\zeta)$, temperature profile $\theta(\zeta)$ and concentration profile $\phi(\zeta)$ which are shown in tables and graphs.

4.2 Mathematical Modeling

It is aimed to analyse the $2D$ MHD flow of non-Newtonian Casson nanofluid past a stretching sheet and porous medium. The flow occupied the space $y > 0$. Furthermore, the flow direction is considered as the x-axis, and the y-axis is normal to it. A Cattaneo-Christov heat flux and thermal radiation are both present during the investigation of energy transport. Moreover, the concentration equation is discussed with the help chemical reaction.

The set of equations describing the flow are as follows.

$$\frac{\partial u}{\partial x} + \frac{\partial v}{\partial y} = 0, \tag{4.1}$$

$$u\frac{\partial u}{\partial x} + v\frac{\partial u}{\partial y} = \nu\left(1 + \frac{1}{\beta}\right)\frac{\partial^2 u}{\partial y^2} - \frac{\nu}{k_1}u - \frac{\sigma B_0^2}{\rho}u, \tag{4.2}$$

$$\begin{aligned} u\frac{\partial T}{\partial x} + v\frac{\partial T}{\partial y} + \lambda_A\Bigg[u\frac{\partial u}{\partial x}\frac{\partial T}{\partial x} + v\frac{\partial v}{\partial y}\frac{\partial T}{\partial y} + u\frac{\partial v}{\partial x}\frac{\partial T}{\partial y} + v\frac{\partial u}{\partial y}\frac{\partial T}{\partial x} + 2uv\frac{\partial^2 T}{\partial x \partial y} \\ + u^2\frac{\partial^2 T}{\partial x^2} + v^2\frac{\partial^2 T}{\partial y^2}\Bigg] = \alpha\left(\frac{\partial^2 T}{\partial y^2}\right) + \tau\left(D_B\frac{\partial C}{\partial y}\frac{\partial T}{\partial x} + \frac{D_T}{T_\infty}\left(\frac{\partial T}{\partial y}\right)^2\right) \\ - \frac{1}{(\rho C_p)}\left(\frac{\partial q_r}{\partial y}\right), \end{aligned} \tag{4.3}$$

$$u\frac{\partial C}{\partial x} + v\frac{\partial C}{\partial y} = D_B\frac{\partial^2 C}{\partial y^2} + \left(\frac{D_T}{T_\infty}\right)\frac{\partial^2 T}{\partial y^2} - K_R(C - C_\infty). \tag{4.4}$$

The associated BCs have been taken as.

$$\left.\begin{aligned} &u = U_w(x) = ax, \quad v = 0, \quad T = T_w, \quad C = C_w, \quad at \quad y = 0, \\ &u \to 0, \quad v \to 0, \quad T \to T_\infty, \quad C \to C_\infty, \quad as \quad y \to \infty. \end{aligned}\right\} \tag{4.5}$$

Following similarity transformation has been used to convert PDEs (4.1)-(4.4) into a system of ODEs.

$$\left.\begin{aligned} &\zeta = \left(\frac{a}{\nu}\right)^{\frac{1}{2}} y, \quad u = axf'(\zeta), \quad v = -(a\nu)^{\frac{1}{2}} f(\zeta), \\ &\theta(\zeta) = \frac{T - T_\infty}{T_w - T_\infty}, \qquad \phi(\zeta) = \frac{C - C_\infty}{C_w - C_\infty}, \end{aligned}\right\} \tag{4.6}$$

where ζ denotes the similarity variable whereas f, θ, and ϕ are the dimensionless velocity, temperature and concentration respectively.

The detailed procedure for the identical satisfaction of (4.1) has been discussed in Chapter 3. The complete procedure for the conversion of (4.2) is also discussed in Chapter 3.

Now, we include below the procedure for the conversion of equation (4.3) into the dimensionless form.

$$(T - T_\infty) = (T_w - T_\infty)\theta(\zeta)$$

$$T = (T_w - T_\infty)\theta(\zeta) + T_\infty. \tag{4.7}$$

$$\frac{\partial T}{\partial x} = 0. \tag{4.8}$$

$$\frac{\partial^2 T}{\partial x \partial y} = 0. \tag{4.9}$$

$$\frac{\partial^2 T}{\partial x^2} = 0. \tag{4.10}$$

$$\begin{aligned}\frac{\partial u}{\partial y} &= axf''(\zeta)\frac{\partial \zeta}{\partial y}\\ &= axf''(\zeta)\left(\frac{a}{\nu}\right)^{\frac{1}{2}}\\ &= \frac{a^{\frac{3}{2}}}{\nu^{\frac{1}{2}}}xf''(\zeta).\end{aligned} \tag{4.11}$$

$$u\frac{\partial u}{\partial x}\frac{\partial T}{\partial x} = axf'(\zeta)(axf''(\zeta))(0)$$

$$u\frac{\partial u}{\partial x}\frac{\partial T}{\partial x} = 0. \tag{4.12}$$

$$\begin{aligned}v\frac{\partial v}{\partial y}\frac{\partial T}{\partial y} &= (-af'(\zeta))\left(-(a\nu)^{\frac{1}{2}}f(\zeta)\right)\left(\left(\frac{a}{\nu}\right)^{\frac{1}{2}}(T_w - T_\infty)\theta'(\zeta)\right)\\ &= a^2(T_w - T_\infty)f(\zeta)f'(\zeta)\theta'(\zeta).\end{aligned} \tag{4.13}$$

$$u\frac{\partial v}{\partial x}\frac{\partial T}{\partial y} = axf'(\zeta)(0)\left(\left(\frac{a}{\nu}\right)^{\frac{1}{2}}(T_w - T_\infty)\theta'(\zeta)\right)$$

$$u\frac{\partial v}{\partial x}\frac{\partial T}{\partial y} = 0. \tag{4.14}$$

$$v\frac{\partial u}{\partial y}\frac{\partial T}{\partial x} = \left(-(a\nu)^{\frac{1}{2}}f(\zeta)\right)\left(\frac{a^{\frac{3}{2}}}{\nu^{\frac{1}{2}}}xf''(\zeta)\right)(0)$$

$$v\frac{\partial u}{\partial y}\frac{\partial T}{\partial x} = 0. \tag{4.15}$$

$$2uv\frac{\partial^2 T}{\partial x \partial y} = 2(axf'(\zeta))\left(-(a\nu)^{\frac{1}{2}}f(\zeta)\right)(0)$$

$$2uv\frac{\partial^2 T}{\partial x \partial y} = 0. \tag{4.16}$$

$$u^2\frac{\partial^2 T}{\partial x^2} = 0. \tag{4.17}$$

$$\begin{aligned} v^2\frac{\partial^2 T}{\partial y^2} &= \left(-(a\nu)^{\frac{1}{2}} f(\zeta)\right)^2 \left(\left(\frac{a}{\nu}\right)(T_w - T_\infty)\theta''(\zeta)\right) \\ &= a^2(T_w - T_\infty) f^2(\zeta)\theta''(\zeta). \end{aligned} \tag{4.18}$$

Adding equations (4.12)-(4.18), we get.

$$\begin{aligned} &u\frac{\partial u}{\partial x}\frac{\partial T}{\partial x} + v\frac{\partial v}{\partial y}\frac{\partial T}{\partial y} + u\frac{\partial v}{\partial x}\frac{\partial T}{\partial y} + v\frac{\partial u}{\partial y}\frac{\partial T}{\partial x} + 2uv\frac{\partial^2 T}{\partial x\partial y} + u^2\frac{\partial^2 T}{\partial x^2} + v^2\frac{\partial^2 T}{\partial y^2} \\ &= 0 + a^2(T_w - T_\infty) f(\zeta) f'(\zeta)\theta'(\zeta) + 0 + 0 + 0 + 0 + a^2(T_w - T_\infty) f^2(\zeta)\theta''(\zeta) \\ &= a^2(T_w - T_\infty) f(\zeta) f'(\zeta)\theta'(\zeta) + a^2(T_w - T_\infty) f^2(\zeta)\theta''(\zeta) \\ &= a^2(T_w - T_\infty)\Big[f(\zeta) f'(\zeta)\theta'(\zeta) + f^2(\zeta)\theta''(\zeta)\Big]. \end{aligned} \tag{4.19}$$

Left hand side of (4.3)

$$\begin{aligned} u\frac{\partial T}{\partial x} + v\frac{\partial T}{\partial y} + \lambda_A\Big[&u\frac{\partial u}{\partial x}\frac{\partial T}{\partial x} + v\frac{\partial v}{\partial y}\frac{\partial T}{\partial y} + u\frac{\partial v}{\partial x}\frac{\partial T}{\partial y} + v\frac{\partial u}{\partial y}\frac{\partial T}{\partial x} + 2uv\frac{\partial^2 T}{\partial x\partial y} \\ &+ u^2\frac{\partial^2 T}{\partial x^2} + v^2\frac{\partial^2 T}{\partial y^2}\Big] = -a(T_w - T_\infty) f(\zeta)\theta'(\zeta) \\ &+ \lambda_A a^2(T_w - T_\infty)\Big[f(\zeta) f'(\zeta)\theta'(\zeta) + f^2(\zeta)\theta''(\zeta)\Big]. \end{aligned} \tag{4.20}$$

Right side of (4.3), we get

$$\begin{aligned} &\alpha\frac{\partial^2 T}{\partial y^2} + \tau\left(D_B\frac{\partial C}{\partial y}\frac{\partial T}{\partial y} + \frac{D_T}{T_\infty}\left(\frac{\partial T}{\partial y}\right)^2\right) - \frac{1}{(\rho Cp)}\frac{\partial q_r}{\partial y} \\ &= \alpha\left(\frac{a}{\nu}\right)(T_w - T_\infty)\theta''(\zeta) + \tau D_B\left(\frac{a}{\nu}\right)(T_w - T_\infty)\theta'(\zeta)(C_w - C_\infty)\phi'(\zeta) \\ &\quad + \tau\frac{D_T}{T_\infty}\left(\frac{a}{\nu}\right)(T_w - T_\infty)^2\theta'^2(\zeta) + \frac{1}{\rho c_p}\left(\frac{16\sigma^* T_\infty^3}{3k^*}\left(\frac{a}{\nu}\right)(T_w - T_\infty)\theta''(\zeta)\right). \end{aligned} \tag{4.21}$$

Comparing (4.20) and (4.21)

$$\begin{aligned} &- a(T_w - T_\infty) f(\zeta)\theta'(\zeta) + \lambda_A a^2(T_w - T_\infty)\Big[f(\zeta) f'(\zeta)\theta'(\zeta) + f^2(\zeta)\theta''(\zeta)\Big] \\ &= \tau D_B\left(\frac{a}{\nu}\right)(T_w - T_\infty)\theta'(\zeta)(C_w - C_\infty)\phi'(\zeta) + \tau\frac{D_T}{T_\infty}\left(\frac{a}{\nu}\right)(T_w - T_\infty)^2\theta'^2(\zeta) \end{aligned}$$

$$
\begin{aligned}
&+\alpha\left(\frac{a}{\nu}\right)(T_w-T_\infty)\theta''(\zeta)+\frac{1}{\rho c_p}\left(\frac{16\sigma^*T_\infty^3}{3k^*}\left(\frac{a}{\nu}\right)(T_w-T_\infty)\theta''(\zeta)\right).\\
\Rightarrow\quad &-af(\zeta)\theta'(\zeta)+\lambda_A a^2\Big[f(\zeta)f'(\zeta)\theta'(\zeta)+f^2(\zeta)\theta''(\zeta)\Big]\\
&=\tau\frac{D_T}{T_\infty}\left(\frac{a}{\nu}\right)(T_w-T_\infty)\theta'^2(\zeta)+\tau D_B\left(\frac{a}{\nu}\right)\theta'(\zeta)(C_w-C_\infty)\phi'(\zeta)\\
&+\frac{a}{\nu}\left(\alpha+\frac{1}{\rho c_p}\left(\frac{16\sigma^*T_\infty^3}{3k^*}\right)\right)\theta''(\zeta).\\
\Rightarrow\quad &-f(\zeta)\theta'(\zeta)+\lambda_A a\Big[f(\zeta)f'(\zeta)\theta'(\zeta)+f^2(\zeta)\theta''(\zeta)\Big]\\
&=\tau\frac{D_T}{T_\infty}\left(\frac{1}{\nu}\right)(T_w-T_\infty)\theta'^2(\zeta)+\tau D_B\left(\frac{1}{\nu}\right)\theta'(\zeta)(C_w-C_\infty)\phi'(\zeta)\\
&+\frac{1}{\nu}\left(\alpha+\frac{1}{\rho c_p}\left(\frac{16\sigma^*T_\infty^3}{3k^*}\right)\right)\theta''(\zeta).\\
\Rightarrow\quad &\frac{1}{\nu}\left(\frac{k}{\rho c_p}+\frac{1}{\rho c_p}\left(\frac{16\sigma^*T_\infty^3}{3k^*}\right)\right)\theta''(\zeta)-\lambda_A a\Big[f(\zeta)f'(\zeta)\theta'(\zeta)+f^2(\zeta)\theta''(\zeta)\Big]\\
&+f(\zeta)\theta'(\zeta)+\frac{\tau D_B(C_w-C_\infty)}{\nu}\theta'(\zeta)\phi'(\zeta)+\frac{\tau D_T(T_w-T_\infty)}{T_\infty\nu}\theta'^2(\zeta)=0\\
\Rightarrow\quad &\frac{k}{\nu\rho c_p}\left(1+\frac{16\sigma^*T_\infty^3}{3k^*k}\right)\theta''(\zeta)-\gamma_1\Big[f(\zeta)f'(\zeta)\theta'(\zeta)+f^2(\zeta)\theta''(\zeta)\Big]\\
&+f(\zeta)\theta'(\zeta)+Nb\theta'(\zeta)\phi'(\zeta)+Nt\theta'^2(\zeta)=0.\\
\Rightarrow\quad &\frac{\alpha}{\nu}\left(1+\frac{4}{3}R\right)\theta''(\zeta)-\gamma_1\Big[f(\zeta)f'(\zeta)\theta'(\zeta)+f^2(\zeta)\theta''(\zeta)\Big]+f(\zeta)\theta'(\zeta)\\
&+Nb\theta'(\zeta)\phi'(\zeta)+Nt\theta'^2(\zeta)=0.\\
\Rightarrow\quad &\frac{1}{Pr}\left(1+\frac{4}{3}R\right)\theta''(\zeta)-\gamma_1\Big(f(\zeta)f'(\zeta)\theta'(\zeta)+f^2(\zeta)\theta''(\zeta)\Big)+f(\zeta)\theta'(\zeta)\\
&+Nb\theta'(\zeta)\phi'(\zeta)+Nt\theta'^2(\zeta)=0. \qquad (4.22)
\end{aligned}
$$

Now, we include below the procedure for the conversion of equation (4.3) into the dimensionless form.

$$
\begin{aligned}
&\phi(\zeta)=\frac{C-C_\infty}{C_w-C_\infty}.\\
&(C_w-C_\infty)=(C-C_\infty)\phi(\zeta)\\
&C=(C_w-C_\infty)\phi(\zeta)+C_\infty. \qquad (4.23)\\
&\frac{\partial^2 C}{\partial y^2}=\left(\frac{a}{\nu}\right)^{\frac{1}{2}}(C_w-C_\infty)\phi''(\zeta)\frac{\partial\zeta}{\partial y}\\
&\qquad=\left(\frac{a}{\nu}\right)(C_w-C_\infty)\phi''(\zeta). \qquad (4.24)
\end{aligned}
$$

Left hand side of (4.4), we get

$$u\frac{\partial C}{\partial x}+v\frac{\partial C}{\partial y}=-a(C_w-C_\infty)f(\zeta)\phi'(\zeta). \tag{4.25}$$

Right hand side of (4.4)

$$\begin{aligned}D_B\frac{\partial^2 C}{\partial y^2}+\frac{D_T}{T_\infty}\frac{\partial^2 T}{\partial y^2}-K_R(C_w-C_\infty)&=D_B\left(\frac{a}{\nu}\right)(C_w-C_\infty)\phi''(\zeta)\\&+\frac{D_T}{T_\infty}\left(\frac{a}{\nu}\right)(T_w-T_\infty)\theta''(\zeta)-K_R(C-C_\infty)\phi(\zeta).\end{aligned} \tag{4.26}$$

Comparing (4.25) and (4.26),

$$\begin{aligned}&-a(C_w-C_\infty)f(\zeta)\phi'(\zeta)=D_B\left(\frac{a}{\nu}\right)(C_w-C_\infty)\phi''(\zeta)\\&+\frac{D_T}{T_\infty}\left(\frac{a}{\nu}\right)(T_w-T_\infty)\theta''(\zeta)-K_R(C-C_\infty)\phi(\zeta).\\\Rightarrow\quad&-af(\zeta)\phi'(\zeta)=D_B\left(\frac{a}{\nu}\right)\phi''(\zeta)+\frac{D_T}{T_\infty}\left(\frac{a}{\nu}\right)\frac{(T_w-T_\infty)}{(C_w-C_\infty)}\theta''(\zeta)-K_R\phi(\zeta).\\\Rightarrow\quad&-f(\zeta)\phi'(\zeta)=D_B\left(\frac{1}{\nu}\right)\phi''(\zeta)+\frac{D_T}{T_\infty}\left(\frac{1}{\nu}\right)\frac{(T_w-T_\infty)}{(C_w-C_\infty)}\theta''(\zeta)-\frac{K_R}{a}\phi(\zeta).\\\Rightarrow\quad&-\frac{\nu}{D_B}f(\zeta)\phi'(\zeta)=\phi''(\zeta)+\frac{D_T}{T_\infty}\frac{(T_w-T_\infty)}{D_B(C_w-C_\infty)}\theta''(\zeta)-\frac{\nu}{D_B}\frac{K_R}{a}\phi(\zeta).\\\Rightarrow\quad&-Scf(\zeta)\phi'(\zeta)=\phi''(\zeta)+\frac{D_T}{T_\infty}\frac{\tau\nu(T_w-T_\infty)}{\tau\nu D_B(C_w-C_\infty)}\theta''(\zeta)-Sc\gamma_2\phi(\zeta).\\\Rightarrow\quad&-Scf(\zeta)\phi'(\zeta)=\phi''(\zeta)+\frac{Nt}{Nb}\theta''(\zeta)-Sc\gamma_2\phi(\zeta).\\\Rightarrow\quad&\phi''(\zeta)+Scf(\zeta)\phi'(\zeta)+\frac{Nt}{Nb}\theta''(\zeta)-Sc\gamma_2\phi(\zeta)=0.\end{aligned} \tag{4.27}$$

The corresponding bc's are coverted into the non-dimensional form through the following procedure.

$$\begin{aligned}&u=U_w(x)=ax, && at\quad y=0.\\\Rightarrow\quad&u=axf'(\zeta), && at\quad \zeta=0.\\\Rightarrow\quad&axf'(\zeta)=ax, && at\quad \zeta=0.\\\Rightarrow\quad&f'(\zeta)=1, && at\quad \zeta=0.\\\Rightarrow\quad&f'(0)=1.\end{aligned}$$

$$
\begin{aligned}
& v = 0, && at \quad y = 0. \\
\Rightarrow \quad & -(a\nu)^{\frac{1}{2}} f(0) = 0, && at \quad \zeta = 0. \\
\Rightarrow \quad & f(0) = 0. && \\
& T = T_w, && at \quad y = 0. \\
\Rightarrow \quad & \theta(\zeta)(T_w - T_\infty) + T_\infty = T_w, && at \quad \zeta = 0. \\
\Rightarrow \quad & \theta(\zeta)(T_w - T_\infty) = (T_w - T_\infty), && at \quad \zeta = 0. \\
\Rightarrow \quad & \theta(\zeta) = 1, && at \quad \zeta = 0. \\
\Rightarrow \quad & \theta(0) = 1. && \\
& C = C_w, && at \quad y = 0. \\
\Rightarrow \quad & \phi(\zeta)(C_w - C_\infty) + C_\infty = C_w, && at \quad \zeta = 0. \\
\Rightarrow \quad & \phi(\zeta)(C_w - C_\infty) = (C_w - C_\infty), && at \quad \zeta = 0. \\
\Rightarrow \quad & \phi(\zeta) = 1, && at \quad \zeta = 0. \\
\Rightarrow \quad & \phi(0) = 1. && \\
& u \to (0), && as \quad y \to \infty. \\
\Rightarrow \quad & af'(\zeta)x \to (0), && as \quad y \to \infty. \\
\Rightarrow \quad & axf'(\zeta) \to (0), && \\
\Rightarrow \quad & f'(\zeta) \to (0), && as \quad \zeta \to \infty. \\
\Rightarrow \quad & f'(\infty) \to 0. && \\
& T \to T_\infty, && as \quad y \to \infty. \\
\Rightarrow \quad & \theta(\zeta)(T_w - T_\infty) + T_\infty \to T_\infty, && \\
\Rightarrow \quad & \theta(\zeta)(T_w - T_\infty) \to 0, && as \quad \zeta \to \infty. \\
\Rightarrow \quad & \theta(\zeta) \to 0, && as \quad \zeta \to \infty. \\
\Rightarrow \quad & \theta(\infty) \to 0. && \\
& C \to C_\infty, && as \quad y \to \infty. \\
\Rightarrow \quad & \phi(\zeta)(C_w - C_\infty) + C_\infty \to C_\infty, && \\
\Rightarrow \quad & \phi(\zeta)(C_w - C_\infty) \to 0, && \\
\Rightarrow \quad & \phi(\zeta) \to 0, && as \quad \zeta \to \infty. \\
\Rightarrow \quad & \phi(\infty) \to 0. &&
\end{aligned}
$$

The final dimensionless form of the governing model, is

$$\left(\frac{1+\beta}{\beta}\right) f'''(\zeta) + f(\zeta)f''(\zeta) - f'^2(\zeta) - (M+K)f'(\zeta) = 0, \tag{4.28}$$

$$\frac{1}{Pr}\left(1+\frac{4}{3}R\right)\theta''(\zeta) - \gamma_1\Big(f(\zeta)f'(\zeta)\theta'(\zeta) + f^2(\zeta)\theta''(\zeta)\Big) + f(\zeta)\theta'(\zeta)$$
$$+ Nb\theta'(\zeta)\phi'(\zeta) + Nt\theta'^2(\zeta) = 0, \tag{4.29}$$

$$\phi''(\zeta) + Scf(\zeta)\phi'(\zeta) + \frac{Nt}{Nb}\theta''(\zeta) - Sc\gamma_2\phi(\zeta) = 0. \tag{4.30}$$

The associated BCs (4.5) in the dimensionless form are:

$$\left.\begin{array}{llll} f(0) = 0, & f'(0) = 1, & \theta(0) = 1, & \phi(0) = 1. \\ f'(\infty) \to 0, & \theta(\infty) \to 0, & \phi(\infty) \to 0. & \end{array}\right\} \tag{4.31}$$

Different parameters used in equations (4.28)-(4.30) are formulated as follows.

$$M = \frac{\sigma B_0^2}{\rho a}, \quad R = \frac{4\sigma^* T_\infty^3}{kk^*}, \quad Nb = \frac{\tau D_B(C_w - C_\infty)}{\nu}, \quad \gamma_1 = \lambda_A a,$$
$$Pr = \frac{\nu}{\alpha}, \quad Sc = \frac{\nu}{D_B}, \quad K = \frac{\nu}{k_1 a}, \quad Nt = \frac{\tau D_T(T_w - T_\infty)}{T_\infty \nu}, \quad \gamma_2 = \frac{K_R}{a}.$$

4.3 Solution Methodology

In order to solve the system of ODEs (4.28) the shooting method has been used. The following notations have been cosidered.

$$f = Y_1, \qquad f' = Y_1' = Y_2, \qquad f'' = Y_1'' = Y_2' = Y_3, \qquad f''' = Y_3'.$$

The following system of first order ODEs is created by converting the momentum equation.

$$\begin{aligned} &Y_1' = Y_2, && Y_1(0) = 0. \\ &Y_2' = Y_3, && Y_2(0) = 1. \\ &Y_3' = \left(\frac{\beta}{1+\beta}\right)\left(-Y_1Y_3 + Y_2^2 + (M+K)Y_2\right), && Y_3(0) = s. \end{aligned}$$

The above IVP will be numerically solved by RK-4. The bounded domain $[0,\ \zeta_\infty]$ has been used in place of the unbounded domain $[0\ ,\ \infty)$ for the numerical results with the observation that it produces an asymptotic covergence of the solution. The missing condition s is to be chosen such that.

$$Y_2(\zeta_\infty, s) = 0.$$

Newton's method will be used to find s. This method has the following iterative scheme.

$$s^{(n+1)} = s^{(n)} - \frac{Y_2(\zeta_\infty, s^{(n)})}{\left(\frac{\partial}{\partial p}(Y_2(\zeta_\infty, s))\right)^{(n)}}.$$

We further introduce the following notations:

$$\frac{\partial Y_1}{\partial s} = Y_4, \qquad \frac{\partial Y_2}{\partial s} = Y_5, \qquad \frac{\partial Y_3}{\partial s} = Y_6.$$

As a result of these new notations, the Newton's iterative scheme gets the form:

$$s^{(n+1)} = s^{(n)} - \frac{Y_2(\zeta_\infty, s^{(n)})}{Y_5(\zeta_\infty, s^{(n)})}.$$

Now differentiating the system of three first order ODEs with respect to s, we get another system of ODEs, as follows.

$$\begin{aligned}
&Y_4' = Y_5, && Y_4(0) = 0.\\
&Y_5' = Y_6, && Y_5(0) = 0.\\
&Y_6' = \left(\frac{\beta}{1+\beta}\right)\left(-Y_4Y_3 - Y_1Y_6 + 2Y_2Y_5 + (M+K)Y_5\right), && Y_6(0) = 1.
\end{aligned}$$

The stopping criteria for the Newton's technique is set as.

$$\mid Y_2(\zeta_\infty, s) \mid < \epsilon,$$

where $\epsilon > 0$ is an arbitrarily small positive number. From now onward ϵ has been taken as 10^{-10}.

Also, for equations (4.29) and (4.30), the following notations have been used.

$$\theta = Z_1, \quad \theta' = Z_2, \quad \theta'' = Z_2', \quad \phi = Z_3, \quad \phi' = Z_4, \quad \phi'' = Z_4',$$
$$A_1 = \left[1 + \frac{4}{3}R\right], \quad A_2 = \left[A_1 - Pr\gamma_1 f^2\right].$$

The system of equations (4.29) and (4.30), can be written in the form of the following first order coupled ODEs.

$$\begin{aligned}
Z_1' &= Z_2, && Z_1(0) = 1.\\
Z_2' &= -\frac{Pr}{A_2}\left[fZ_2 - \gamma_1 ff'Z_2 + NbZ_2Z_4 + NtZ_2^2\right], && Z_2(0) = p.\\
Z_3' &= Z_4, && Z_3(0) = 1.\\
Z_4' &= \gamma_2 ScZ_3 - ScfY_4 + \frac{Nt}{Nb}\left[\frac{Pr}{A_2}\left[fZ_2 - \gamma_1 ff'Z_2 + NbZ_2Z_4 + NtZ_2^2\right]\right],\\
& && Z_4(0) = q.
\end{aligned}$$

The RK-4 technique will be used to numerically solve the initial value problem mentioned above. The missing conditions p and q in the above system of equations must be selected in such a way.

$$Z_1(\zeta_\infty, p, q) = 0, \qquad Z_3(\zeta_\infty, p, q) = 0.$$

To solve the above algebaric equations, we apply the Newton's method which has the following scheme.

$$\begin{bmatrix} p \\ q \end{bmatrix}^{(n+1)} = \begin{bmatrix} p \\ q \end{bmatrix}^{(n)} - \left(\begin{bmatrix} \frac{\partial Z_1}{\partial p} & \frac{\partial Z_1}{\partial q} \\ \frac{\partial Z_3}{\partial p} & \frac{\partial Z_3}{\partial q} \end{bmatrix}^{-1} \begin{bmatrix} Z_1 \\ Z_3 \end{bmatrix} \right)^{(n)}$$

Now, introduce the following notations,

$$\frac{\partial Z_1}{\partial p} = Z_5, \qquad \frac{\partial Z_2}{\partial p} = Z_6, \qquad \frac{\partial Z_3}{\partial p} = Z_7, \qquad \frac{\partial Z_4}{\partial l} = Z_8.$$
$$\frac{\partial Z_1}{\partial q} = Z_9, \qquad \frac{\partial Z_2}{\partial q} = Z_{10}, \qquad \frac{\partial Z_3}{\partial q} = Z_{11}, \qquad \frac{\partial Z_4}{\partial q} = Z_{12}.$$

As the result of these new notations, the Newton's iterative scheme gets the form.

$$\begin{bmatrix} p \\ q \end{bmatrix}^{(n+1)} = \begin{bmatrix} p \\ q \end{bmatrix}^{(n)} - \left(\begin{bmatrix} Z_5 & Z_9 \\ Z_7 & Z_{11} \end{bmatrix}^{-1} \begin{bmatrix} Z_1 \\ Z_3 \end{bmatrix} \right)^{(n)}$$

Now differentiating the system of four first order ODEs with respect to p, and q we get another system of ODEs, as follows.

$$Z_5' = Z_6, \qquad Z_5(0) = 0.$$

$$Z_6' = -\frac{Pr}{A_2}\Big[fZ_6 - \gamma_1 ff'Z_6 + Nb(Z_6Z_4 + Z_2Z_8) + 2NtZ_2Z_6\Big], \qquad Z_6(0) = 1.$$

$$Z_7' = Z_8, \qquad Z_7(0) = 0.$$

$$Z_8' = \gamma_2 ScZ_7 - ScfY_8 + \frac{Nt}{Nb}\Bigg[\frac{Pr}{A_2}\Big[fZ_6 - \gamma_1 ff'Z_6 + Nb(Z_6Z_4 + Z_2Z_8) + 2NtZ_2Z_6\Big]\Bigg], \qquad Z_8(0) = 0.$$

$$Z_9' = Z_{10}, \qquad Z_9(0) = 0.$$

$$Z_{10}' = -\frac{Pr}{A_2}\Big[fZ_{10} - \gamma_1 ff'Z_{10} + Nb(Z_{10}Z_4 + Z_2Z_{12}) + 2NtZ_2Z_{10}\Big], \qquad Z_{10}(0) = 0.$$

$$Z_{11}' = Z_{12}, \qquad Z_{11}(0) = 0.$$

$$Z_{12}' = \gamma_2 Scff'Z_{12} - ScfY_{12} + \frac{Nt}{Nb}\Bigg[\frac{Pr}{A_2}\Big[fZ_{10} - \gamma_1 ff'Z_{10} + Nb(Z_{10}Z_4 + Z_2Z_{12}) + 2NtZ_2Z_{10}\Big]\Bigg], \qquad Z_{12}(0) = 1.$$

The stopping criteria for the Newton's technique is set as.

$$max\{|Z_1(\zeta_\infty, p, q)|, |Z_3(\zeta_\infty, p, q)|\} < \epsilon.$$

4.4 Representation of Graphs and Tables

A detailed explanation of the numerical results in the form of figures and tables has been discussed. The main focus of this section will be on the impact of different parameters on the velocity $f'(\zeta)$, temperatture $\theta(\zeta)$ and concentration distribution $\phi(\zeta)$. The impact of different factors like magnetic parameter M, thermal radiation R and Schmidt number Sc is observed graphically. Numerical outcomes of the local Nusselt number and local Sherwood number for the distinct values of some fixed parameters are shown in Tables 4.1. The missing initial conditions $\theta(\zeta)$ and $\phi(\zeta)$ can be chosen from I_g and I_h. It is remarkable that the intervals mentioned offer a considerable flexibility for the choice of the initial guess.

Figures 4.1 and 4.2 show the impact of Casson fluid parameter β on the velocity profile $f'(\zeta)$ and temperature profile $\theta(\zeta)$. By increasing the value of β, the velocity of the fluid decreases and temperature increases. When Casson fluid parameter β is incresed, the yield stress is decreased and Casson acts like Newtonain fluid. Furthermore, it is inferred that the velocity of Casson fluid exceeds that of the Newtonian fluid.

Figure 4.3 displays the impact of M on the velocity distribution. By rising the values of M, the velocity distribution shows a decreasing behavior due to the presence of Lorentz force. Figure 4.4 describes the impact of M on the temperature distribution. The temperature distribution expands by rising the values of the magnetic parameter M.

Figures 4.5 and 4.6 illustrate the impact of Nb on the dimensionless temperature $\theta(\zeta)$ and concentration distribution $\phi(\zeta)$. The behavior of temperature distribution is increased and concentration profile is decreased due to the accelerating values of Nb.

Figure 4.7 shows the impact of thermal radiation R on the temperature distribution $\theta(\zeta)$. By enhancing the values of R, the temperature distribution $\theta(\zeta)$ is increased. Figure 4.8 shows the influencee of the relaxation time parameter γ_1 on the temperature proflie $\theta(\zeta)$. An increment is noticed in the temperature distribution by rising the values of the relaxation time parameter γ_1.

Figure 4.9 depicts the effect of the Schmidt number Sc on the concentration distribution $\phi(\zeta)$. This behaviour is caused by the inverse relationship between the Schmidt number and mass diffusion rate as a result, with larger Schmidt number Sc, the mass diffusivity process slows down, causing the concentration to decrease and the concentration boundary layer thickness to decrease. Figure 4.10 displays the impact of chemical reaction parameter γ_2, on the concentration distribution $\phi(\zeta)$. The concentration profile is similarly influenced by the chemical reaction parameter γ_2. Raising the value of chemical reaction parameter γ_2 decreases the concentration profile $\phi(\zeta)$.

TABLE 4.1: Results of $-(Re_x)^{-\frac{1}{2}}Nu_x$ and $-(Re_x)^{-\frac{1}{2}}Sh_x$ with some fixed parameters $\gamma_1 = 0.1$, $Pr = 7.0$, $Sc = 0.1$, $K = 0.3$.

M	R	β	Nb	Nt	γ_2	$-(Re_x)^{-\frac{1}{2}}Nu_x$	$-(Re_x)^{-\frac{1}{2}}Sh_x$	I_g	I_h
0.2	0.25	0.5	0.1	0.1	0.1	1.564984	-1.132723	[-2.0, 2.0]	[-2.0, 3.0]
0.3						1.560107	-1.129455	[-2.0, 2.5]	[-2.0, 3.0]
0.4						1.555348	-1.126216	[-2.0, 2.5]	[-2.0, 2.0]
0.5						1.550699	-1.123005	[-2.5, 2.5]	[-1.0, 2.0]
0.2	1.0					1.170680	-0.746021	[-3.0, 2.5]	[-2.0, 4.0]
	2.0					0.914570	-0.496707	[-3.0, 5.5]	[-1.0, 2.5]
	4.0					0.666753	-0.257157	[-2.0, 2.5]	[-2.0, 2.0]
	0.25	1.0				1.530931	-1.108910	[-2.0, 2.5]	[-2.0, 2.0]
		1.5				1.512843	-1.095336	[-5.0, 2.0]	[-3.0, 1.0]
		2.0				1.501510	-1.086565	[-2.5, 2.0]	[-4.0, 3.0]
		2.5				1.493719	-1.080428	[-3.0, 2.0]	[-2.5, 1.0]
		3.0				1.485480	-1.0800120	[-3.0, 2.0]	[-2.5, 1.0]
		0.5	0.2			1.488931	-0.412639	[-1.0, 2.5]	[-1.0, 2.0]
			0.3			1.414460	-0.173146	[-2.5, 2.5]	[-2.0, 2.5]
			0.4			1.341623	-0.053813	[-3.0, 2.0]	[-2.0, 2.0]
			0.1	0.2		1.496339	-2.361572	[-1.5, 2.5]	[-2.5, 2.5]
				0.3		1.429276	-3.459243	[-2.0, 2.5]	[-2.0, 2.0]
				0.4		1.363825	-4.430650	[-2.0, 2.5]	[-2.0, 2.0]
				0.5		1.301121	-4.429145	[-2.0, 2.5]	[-2.0, 2.0]
					0.2	1.555783	-1.092207	[-2.0, 2.5]	[-2.0, 2.0]
					0.4	1.538746	-1.016528	[-3.0, 2.5]	[-3.0, 2.5]
					0.6	1.523276	-0.947014	[-2.0, 2.5]	[-2.0, 2.0]
					0.8	1.509127	-0.882721	[-1.0, 3.0]	[-2.0, 2.0]

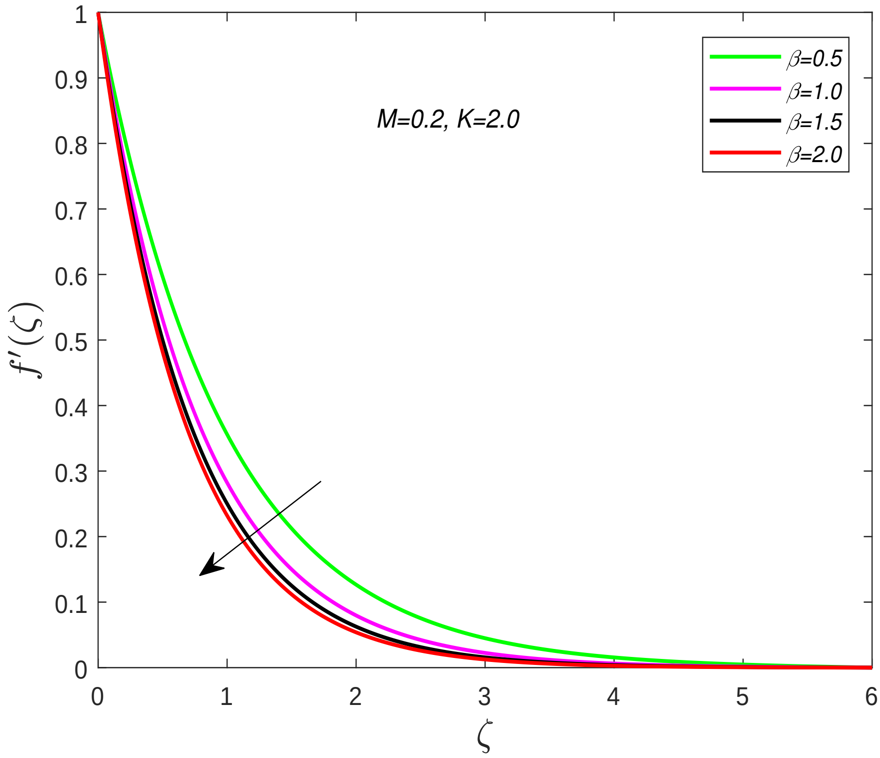

FIGURE 4.1: Velocity profile $f'(\zeta)$ due to change in β.

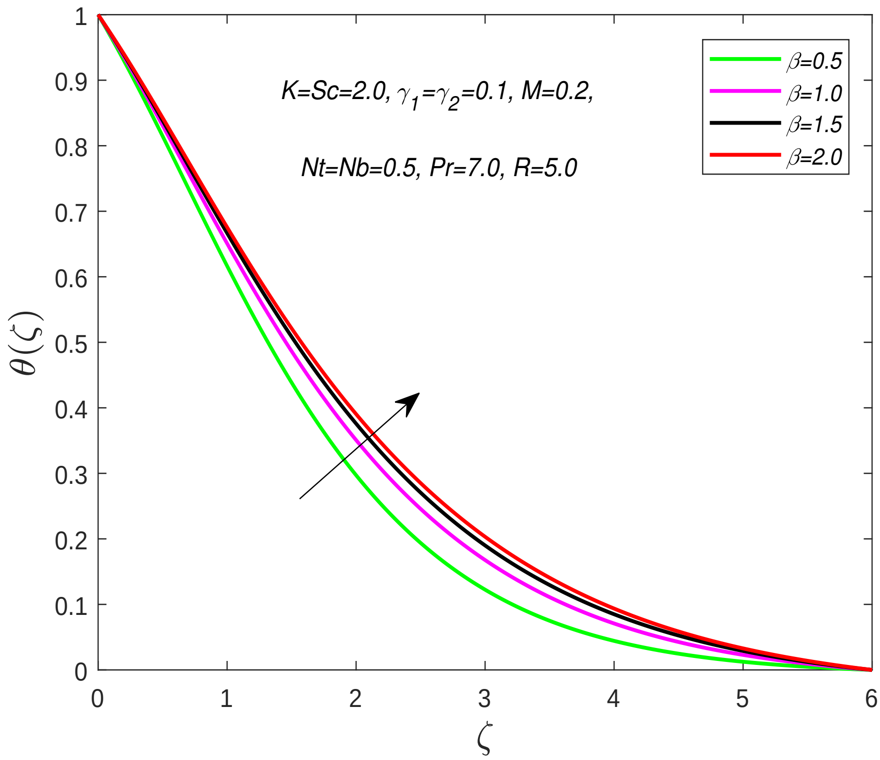

FIGURE 4.2: Temperature profile $\theta(\zeta)$ due to change in β.

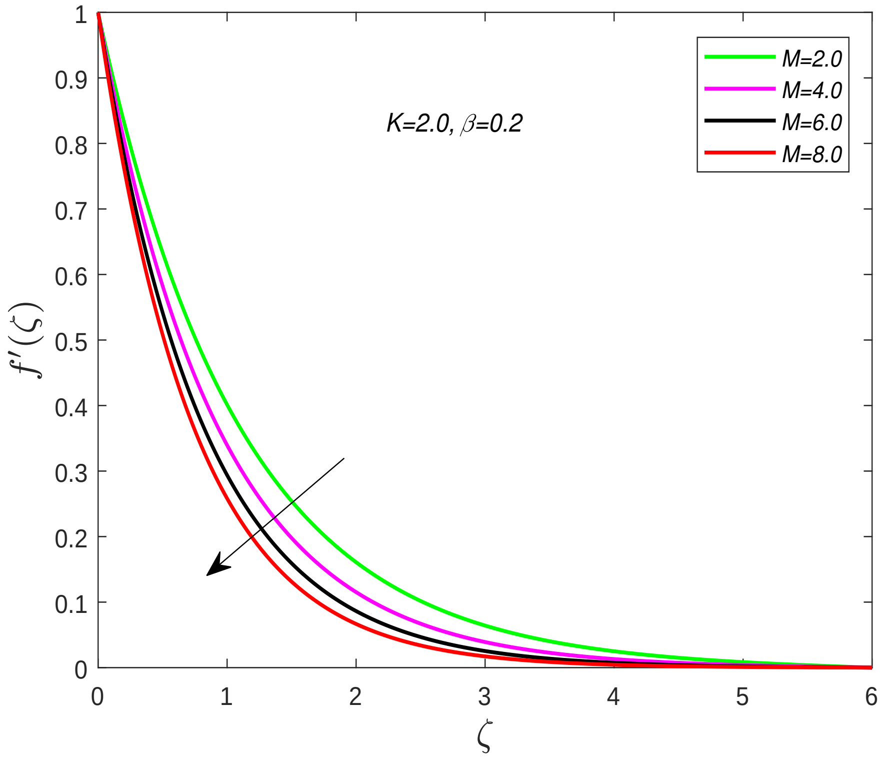

FIGURE 4.3: Velocity profile $f'(\zeta)$ due to change in M.

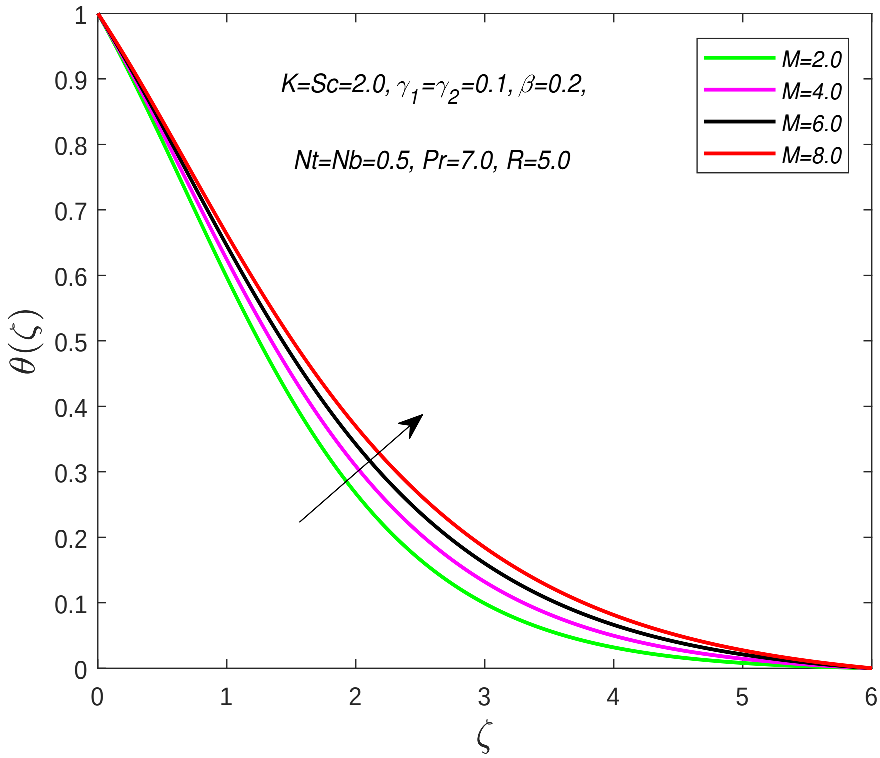

FIGURE 4.4: Temperature profile $\theta(\zeta)$ due to change in M.

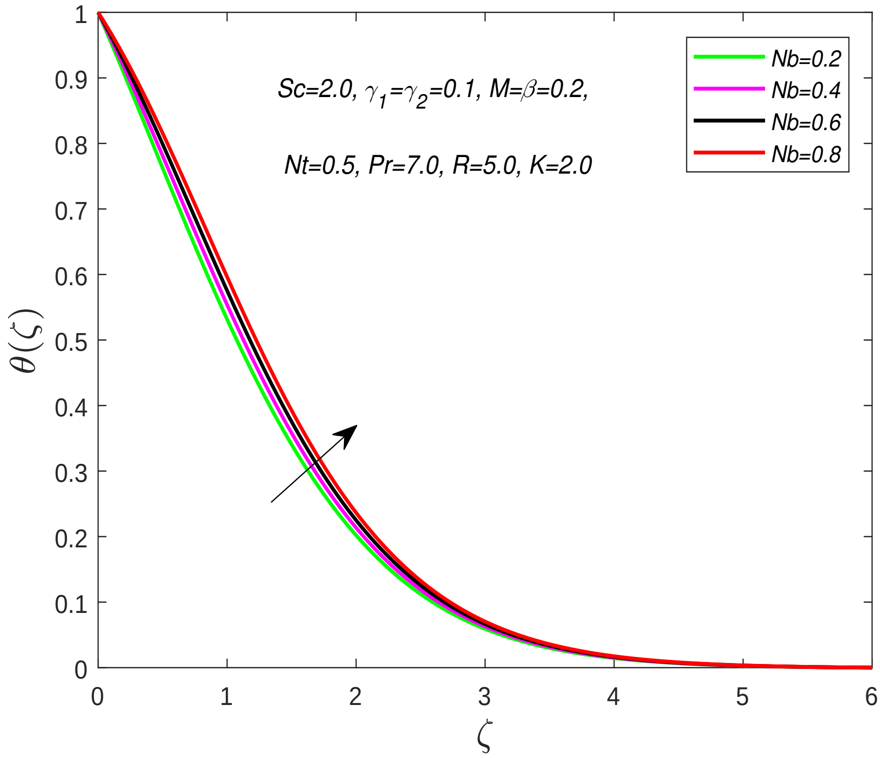

FIGURE 4.5: Temperature profile $\theta(\zeta)$ due to change in Nb.

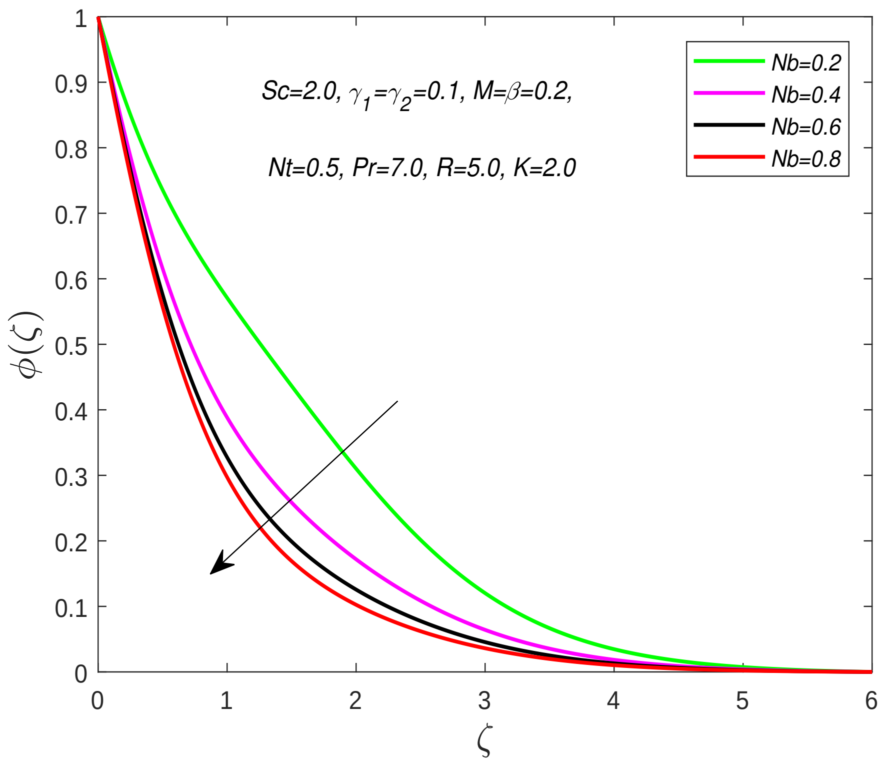

FIGURE 4.6: Concentration profile $\phi(\zeta)$ due to change in Nb.

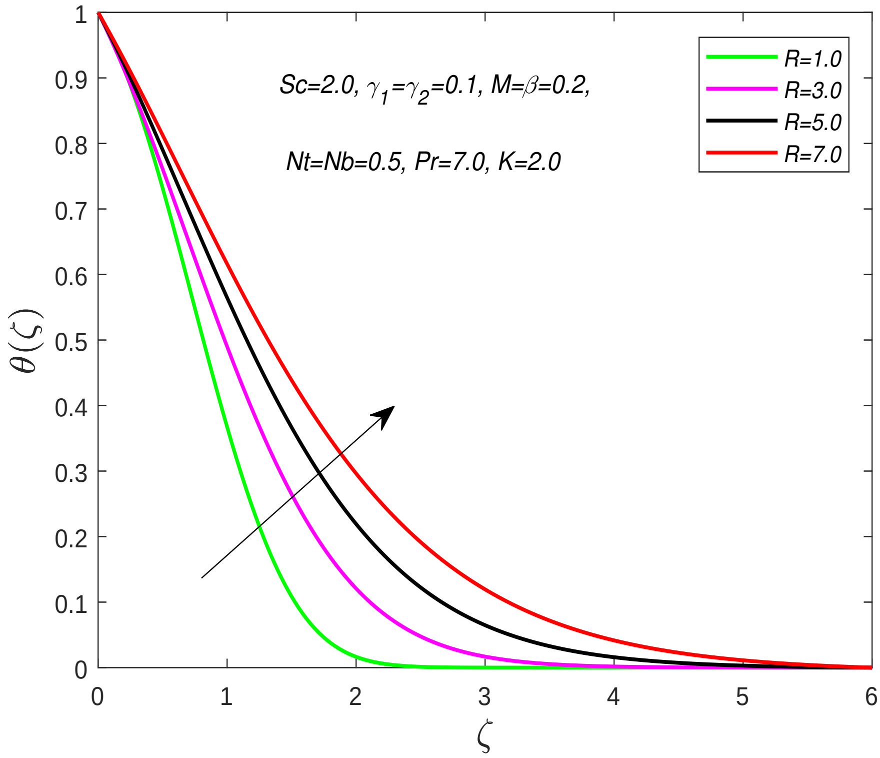

FIGURE 4.7: Temperature profile $\theta(\zeta)$ due to change in R.

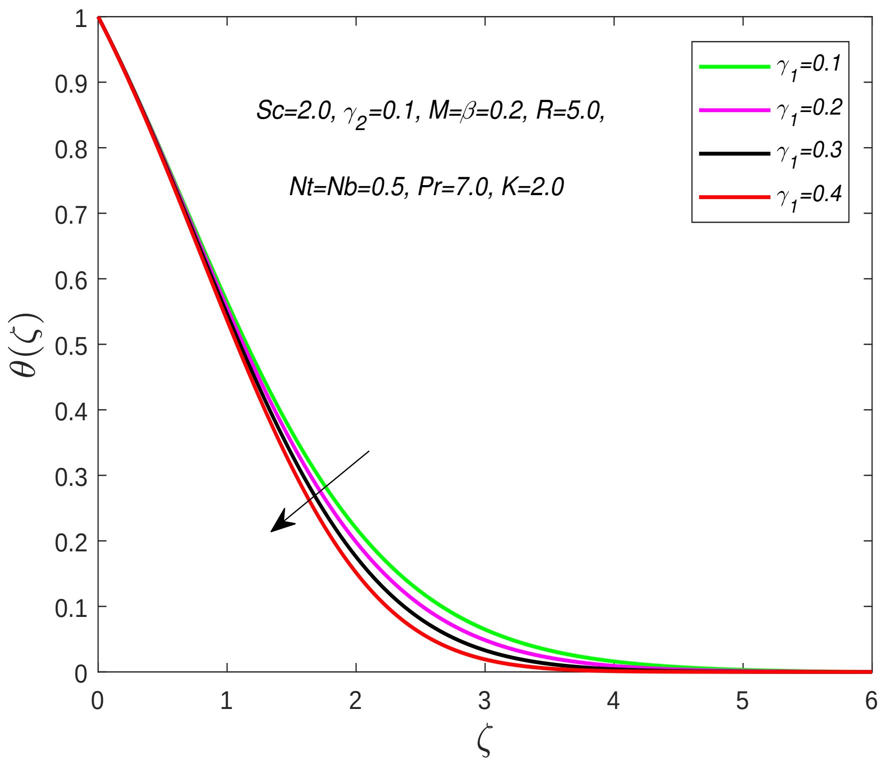

FIGURE 4.8: Temperature profile $\theta(\zeta)$ due to change in γ_1.

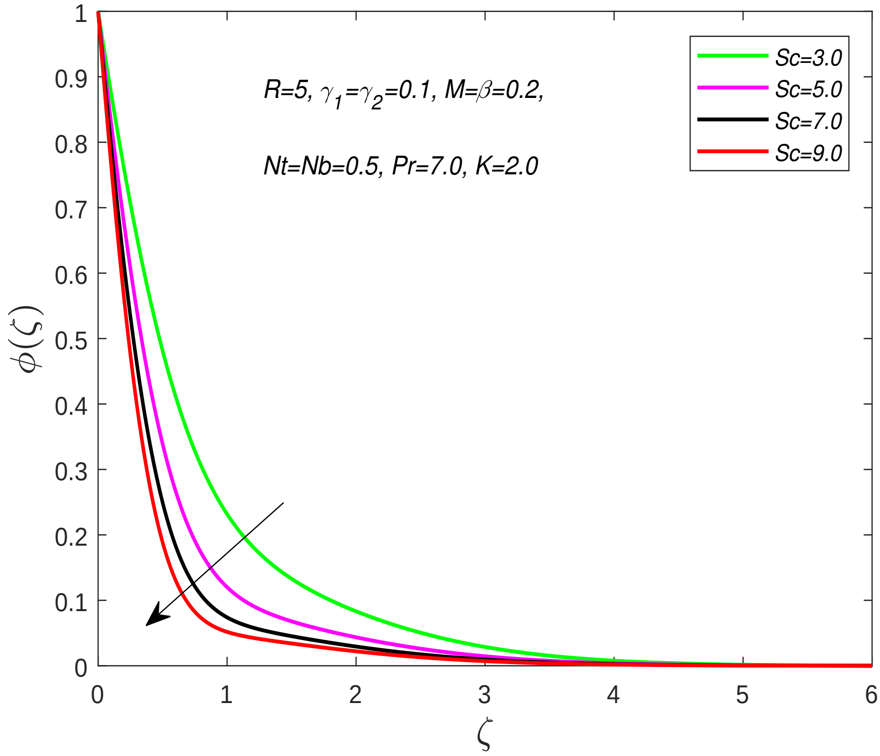

FIGURE 4.9: Concentration profile $\phi(\zeta)$ due to change in Sc.

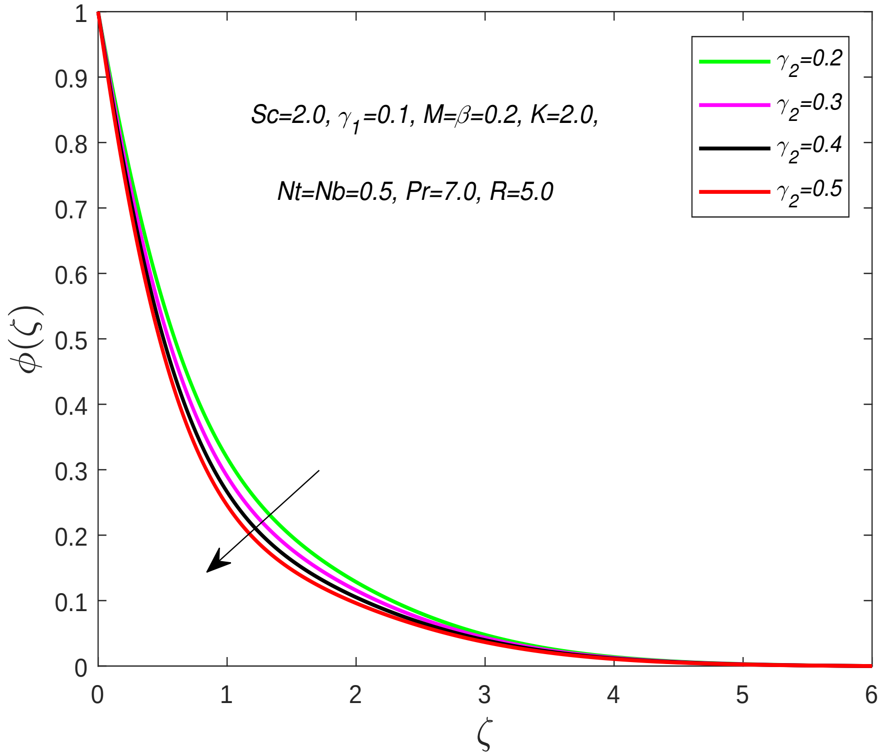

FIGURE 4.10: Concentration profile $\phi(\zeta)$ due to change in γ_2.

Chapter 5

Conclusion

In this thesis, the work of Kho et al. [49] is reviewed and extended with the effect of Cattaneo-Christov heat flux model and chemical reaction. First of all, the governing nonlinear PDEs are converted into a system of dimensionless ODEs by utilizing the appropriate transformations. The shooting technique has been used for the calculation of numerical results along with $RK4$. Using different values of the governing physical parameters, the results are presented in the form of table and graph for $f'(\zeta)$, $\theta(\zeta)$ and $\phi(\zeta)$ profiles. The achievements of the current research can be summarized as below:

- The temperature profile rises while the velocity profile falls when M is increased.
- For the enhancing values of R, the temperature distribution is increased.
- The velocity profile is decreased due to the increasing values of the Casson fluid paramater β.
- Increasing the magnetic parameter M results in a rise in the skin friction coefficent.
- Ascending values of Nt cause the Nusselt number to decrease.
- With a rise in Nb, the temperature profile increases.

- Due to the ascending values of β, the numerical values of skin friction coefficent C_f is increased.

- The rise in values of the relaxation time parameter γ_1 results in an decrease in the temperature profile.

- Due to the ascending values of the chemical reaction parameter γ_2, the values of Nu_x are decreased while Sh_x is increased.

Bibliography

[1] S. Choi, D. Singer, H. Wang, *et al.*, "Developments and applications of non-Newtonian flows," *ASME FED*, vol. 66, pp. 99–105, 1995.

[2] N. A. Yacob, A. Ishak, I. Pop, and K. Vajravelu, "Boundary layer flow past a stretching/shrinking surface beneath an external uniform shear flow with a convective surface boundary condition in a nanofluid," *Nanoscale Research Letters*, vol. 6, no. 1, pp. 1–7, 2011.

[3] A. J. Chamkha and S. El-Kabeir, "Unsteady heat and mass transfer by MHD mixed convection flow over an impulsively stretched vertical surface with chemical reaction and Soret and Dufour effects," *Chemical Engineering Communications*, vol. 200, no. 9, pp. 1220–1236, 2013.

[4] A. E. N. Mahdy, F. M. Hady, and H. A. Nabwey, "Unsteady homogeneous-heterogeneous reactions in MHD nanofluid mixed convection flow past a stagnation point of an impulsively rotating sphere," *Thermal Science*, vol. 25, no. 1 Part A, pp. 243–256, 2021.

[5] R. Pal, "A novel method to determine the thermal conductivity of interfacial layers surrounding the nanoparticles of a nanofluid," *Nanomaterials*, vol. 4, no. 4, pp. 844–855, 2014.

[6] M. Bahiraei, M. Jamshidmofid, and M. Goodarzi, "Efficacy of a hybrid nanofluid in a new microchannel heat sink equipped with both secondary channels and ribs," *Journal of Molecular Liquids*, vol. 273, pp. 88–98, 2019.

[7] M. H. Bahmani, G. Sheikhzadeh, M. Zarringhalam, O. A. Akbari, A. A. Alrashed, G. A. S. Shabani, and M. Goodarzi, "Investigation of turbulent

heat transfer and nanofluid flow in a double pipe heat exchanger," *Advanced Powder Technology*, vol. 29, no. 2, pp. 273–282, 2018.

[8] J. Buongiorno, "Convective transport in nanofluids," *Journal of Heat Transfer*, vol. 128, no. 3, pp. 240–250, 2006.

[9] R. K. Tiwari and M. K. Das, "Heat transfer augmentation in a two-sided lid-driven differentially heated square cavity utilizing nanofluids," *International Journal of Heat and Mass Transfer*, vol. 50, no. 9-10, pp. 2002–2018, 2007.

[10] J.-C. Yang, F.-C. Li, W.-W. Zhou, Y.-R. He, and B.-C. Jiang, "Experimental investigation on the thermal conductivity and shear viscosity of viscoelastic-fluid-based nanofluids," *International Journal of Heat and Mass Transfer*, vol. 55, no. 11-12, pp. 3160–3166, 2012.

[11] Khan and Pop, "Boundary-layer flow of a nanofluid past a stretching sheet," *International Journal of Heat and Mass Transfer*, vol. 53, no. 11-12, pp. 2477–2483, 2010.

[12] F. M. Hady, F. S. Ibrahim, S. M. Abdel-Gaied, and M. R. Eid, "Radiation effect on viscous flow of a nanofluid and heat transfer over a nonlinearly stretching sheet," *Nanoscale Research Letters*, vol. 7, no. 1, pp. 1–13, 2012.

[13] C. Wang, "Free convection on a vertical stretching surface," *Journal of Applied Mathematics and Mechanics*, vol. 69, no. 11, pp. 418–420, 1989.

[14] S. Nadeem, R. U. Haq, and Z. Khan, "Numerical solution of non-Newtonian nanofluid flow over a stretching sheet," *Applied Nanoscience*, vol. 4, no. 5, pp. 625–631, 2014.

[15] B. Prasannakumara, B. Gireesha, R. S. Gorla, and M. Krishnamurthy, "Effects of chemical reaction and nonlinear thermal radiation on Williamson nanofluid slip flow over a stretching sheet embedded in a porous medium," *Journal of Aerospace Engineering*, vol. 29, no. 5, p. 04016019, 2016.

[16] R. Vijayaragavan and S. Karthikeyan, "Hall current effect on chemically reacting MHD Casson fluid flow with Dufour effect and thermal radiation,"

Asian Journal of Applied Science and Technology, vol. 2, no. 2, pp. 228–245, 2018.

[17] T. Hayat, S. Shehzad, and A. Alsaedi, "Soret and Dufour effects on magnetohydrodynamic MHD flow of Casson fluid," *Applied Mathematics and Mechanics*, vol. 33, no. 10, pp. 1301–1312, 2012.

[18] J. Venkatesan, D. Sankar, K. Hemalatha, and Y. Yatim, "Mathematical analysis of Casson fluid model for blood rheology in stenosed narrow arteries," *Journal of Applied Mathematics*, vol. 2013, pp. 1–11, 2013.

[19] S. Pramanik, "Casson fluid flow and heat transfer past an exponentially porous stretching surface in presence of thermal radiation," *Ain Shams Engineering Journal*, vol. 5, no. 1, pp. 205–212, 2014.

[20] M. Mustafa and J. A. Khan, "Model for flow of Casson nanofluid past a non-linearly stretching sheet considering magnetic field effects," *AIP Advances*, vol. 5, no. 7, p. 077148, 2015.

[21] M. Afikuzzaman, M. Ferdows, and M. M. Alam, "Unsteady MHD Casson fluid flow through a parallel plate with Hall current," *Procedia Engineering*, vol. 105, pp. 287–293, 2015.

[22] M. I. Khan, M. Waqas, T. Hayat, and A. Alsaedi, "A comparative study of Casson fluid with homogeneous-heterogeneous reactions,," *Journal of Colloid and Interface Science,*, vol. 498, pp. 85–90, 2017.

[23] A. Kamran, S. Hussain, M. Sagheer, and N. Akmal, "A numerical study of magnetohydrodynamics flow in Casson nanofluid combined with Joule heating and slip boundary conditions," *Results in Physics*, vol. 7, pp. 3037–3048, 2017.

[24] Sarveshanand and A. K. Singh, "Magnetohydrodynamic free convection between vertical parallel porous plates in the presence of induced magnetic field," *Springer Plus*, vol. 4, no. 1, pp. 1–13, 2015.

[25] K. Madhura and S. Iyengar, "Impact of heat and mass transfer on mixed convective flow of nanofluid through porous medium," *International Journal*

of Applied and Computational Mathematics, vol. 3, no. 1, pp. 1361–1384, 2017.

[26] F. Mabood, W. Khan, and A. M. Ismail, "MHD boundary layer flow and heat transfer of nanofluids over a nonlinear stretching sheet," *Journal of Magnetism and Magnetic Materials*, vol. 374, pp. 569–576, 2015.

[27] W. Ibrahim, B. Shankar, and M. M. Nandeppanavar, "MHD stagnation point flow and heat transfer due to nanofluid towards a stretching sheet," *International Journal of Heat and Mass Transfer*, vol. 56, no. 1-2, pp. 1–9, 2013.

[28] M. Bhatti, M. Arain, A. Zeeshan, R. Ellahi, and M. Doranehgard, "Swimming of gyrotactic microorganism in MHD Williamson nanofluid flow between rotating circular plates embedded in porous medium," *Journal of Energy Storage*, vol. 45, p. 103511, 2022.

[29] Y. Xuan and Q. Li, "Investigation on convective heat transfer and flow features of nanofluids," *Heat transfer*, vol. 125, no. 1, pp. 151–155, 2003.

[30] B. K. Jha and B. Aina, "Role of induced magnetic field on MHD natural convection flow in vertical microchannel formed by two electrically nonconducting infinite vertical parallel plates," *Alexandria Engineering Journal*, vol. 55, no. 3, pp. 2087–2097, 2016.

[31] M. Sheikholeslami, D. D. Ganji, M. Y. Javed, and R. Ellahi, "Effect of thermal radiation on magnetohydrodynamics nanofluid flow and heat transfer by means of two phase model," *Journal of Magnetism and Magnetic Materials*, vol. 374, pp. 36–43, 2015.

[32] V. Poply, P. Singh, and A. Yadav, "Stability analysis of MHD outer velocity flow on a stretching cylinder," *Alexandria Engineering Journal*, vol. 57, no. 3, pp. 2077–2083, 2018.

[33] A. J. Chamkha and A. Aly, "MHD free convection flow of a nanofluid past a vertical plate in the presence of heat generation or absorption effects," *Chemical Engineering Communications*, vol. 198, no. 3, pp. 425–441, 2010.

[34] S. E. Ahmed, A. K. Hussein, H. A. Mohammed, and S. Sivasankaran, "Boundary layer flow and heat transfer due to permeable stretching tube in the presence of heat source/sink utilizing nanofluids," *Applied Mathematics and Computation*, vol. 238, pp. 149–162, 2014.

[35] B. Ganga, S. M. Y. Ansari, N. V. Ganesh, and A. A. Hakeem, "MHD radiative boundary layer flow of nanofluid past a vertical plate with internal heat generation/absorption, viscous and ohmic dissipation effects," *Journal of the Nigerian Mathematical Society*, vol. 34, no. 2, pp. 181–194, 2015.

[36] A. Kasaeian, R. Daneshazarian, O. Mahian, L. Kolsi, A. J. Chamkha, S. Wongwises, and I. Pop, "Nanofluid flow and heat transfer in porous media: a review of the latest developments," *International Journal of Heat and Mass Transfer*, vol. 107, pp. 778–791, 2017.

[37] I. Sumirat, Y. Ando, and S. Shimamura, "Theoretical consideration of the effect of porosity on thermal conductivity of porous materials," *Journal of Porous Materials*, vol. 13, no. 3, pp. 439–443, 2006.

[38] R. A. Mahdi, H. Mohammed, K. Munisamy, and N. Saeid, "Review of convection heat transfer and fluid flow in porous media with nanofluid," *Renewable and Sustainable Energy Reviews*, vol. 41, pp. 715–734, 2015.

[39] E. Magyari and A. J. Chamkha, "Combined effect of heat generation or absorption and first order chemical reaction on micropolar fluid flows over a uniformly stretched permeable surface," *International Journal of Thermal Sciences*, vol. 49, no. 9, pp. 1821–1828, 2010.

[40] K. Das, "Effect of chemical reaction and thermal radiation on heat and mass transfer flow of MHD micropolar fluid in a rotating frame of reference," *Journal of Heat and Mass Transfer*, vol. 54, no. 15-16, pp. 3505–3513, 2011.

[41] A. J. Chamkha and A. Rashad, "Unsteady heat and mass transfer by MHD mixed convection flow from a rotating vertical cone with chemical reaction and Soret and Dufour effects," *The Canadian Journal of Chemical Engineering*, vol. 92, no. 4, pp. 758–767, 2014.

[42] R. W. Fox, A. McDonald, and P. Pitchard, *Introduction to Fluid Mechanics*. 2006.

[43] R. Bansal, *A Textbook of Fluid Mechanics and Hydraulic Machines*. Laxmi publications, 2004.

[44] J. N. Reddy and D. K. Gartling, *The Finite Element Method in Heat Transfer and Fluid Dynamics*. CRC press, 2010.

[45] P. A. Davidson and A. Thess, *Magnetohydrodynamics*, vol. 418. Springer Science & Business Media, 2002.

[46] M. Gad-el Hak, *Frontiers in Experimental Fluid Mechanics*, vol. 46. Springer Science & Business Media, 2013.

[47] R. W. Lewis, P. Nithiarasu, and K. N. Seetharamu, *Fundamentals of the Finite Element Method for Heat and Fluid Flow*. John Wiley & Sons, 2004.

[48] J. Kunes, *Dimensionless Physical Quantities in Science and Engineering*. Elsevier, 2012.

[49] Y. B. Kho, A. Hussanan, N. M. Sarif, Z. Ismail, and M. Z. Salleh, "Thermal radiation effects on MHD with flow heat and mass transfer in Casson nanofluid over a stretching sheet," in *MATEC Web of Conferences*, vol. 150, p. 06036, EDP Sciences, 2018.